Ad Hoc Networks (an Elsevier Journal), accepted for publication

An Approximation to the QoS Aware Throughput Region of a Tree Network under IEEE 802.15.4 CSMA/CA with Application to Wireless Sensor Network Design

Abhijit Bhattacharya[a], Anurag Kumar[a]

[a]*Dept. of Electrical Communication Engineering*
Indian Institute of Science, Bangalore, 560012, India

Abstract

In the context of wireless sensor networks, we are motivated by the design of a tree network spanning a set of source nodes that generate packets, a set of additional relay nodes that only forward packets from the sources, and a data sink. We assume that the paths from the sources to the sink have bounded hop count, that the nodes use the IEEE 802.15.4 CSMA/CA for medium access control, and that there are no hidden terminals. In this setting, starting with a set of simple fixed point equations, we derive explicit conditions on the packet generation rates at the sources, so that the tree network approximately provides certain quality of service (QoS) such as end-to-end delivery probability and mean delay. The structures of our conditions provide insight on the dependence of the network performance on the arrival rate vector, *and the topological properties of the tree network*. Our numerical experiments suggest that our approximations are able to capture a significant part of the QoS aware throughput region (of a tree network), that is adequate for many sensor network applications. Furthermore, for the special case of equal arrival rates, default backoff parameters, and for a range of values of target QoS, we show that among all path-length-bounded trees (spanning a given set of sources and the data sink) that meet the conditions derived in the paper, a shortest path tree achieves the maximum throughput.

Keywords: Throughput optimal network design, wireless sensor networks, QoS based design of wireless sensor networks, Throughput region of CSMA/CA, design of multihop CSMA networks

1. Introduction

Our work in this paper is motivated by the following broad problem of designing multi-hop ad hoc wireless networks that utilise IEEE 802.15.4 CSMA/CA as the medium access control. Given a network graph over a set of sensor nodes (also called sources), a set of potential relay locations, and a data sink (also called base station (BS)), where each link meets a certain target quality requirement, the problem is to extract from this graph, a hop length bounded[1] tree topology connecting the sensors to the BS, such that the resulting tree provides certain quality of

[☆]This work was supported by the Department of Electronics and Information Technology under the Automation Systems Technology (ASTEC) program, and by the Department of Science and Technology via a J.C. Bose Fellowship.

Email addresses: abhijit@ece.iisc.ernet.in (Abhijit Bhattacharya), anurag@ece.iisc.ernet.in (Anurag Kumar)

[1]For a discussion of why such a hop count bound is needed, see [1, 2]

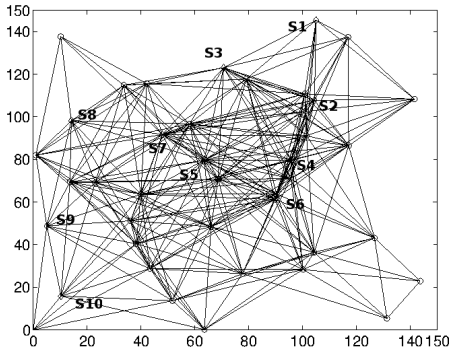

Figure 1: A network graph over 10 sources (labelled $S1, S2, \cdots, S10$) and 30 potential relay locations (the unlabeled vertices); the base station (BS) is at (0,0); each edge is assumed to have a packet error rate of no more than 2%. There are no hidden nodes.

service (QoS), typically expressed in terms of a bound on the packet delivery probability and/or on the mean packet delay, *while also achieving a large throughput region.*

As an example, consider the network graph shown in Figure 1 over 10 sensors, 30 potential relay locations (the unlabeled vertices), and a BS at $(0,0)$; the links in the network have a worst case packet error rate of 2%. Suppose that the nodes use IEEE 802.15.4 CSMA/CA, and that all the nodes are within carrier sense range of one another. The problem is to obtain from this graph (by deploying relays at a subset of the potential locations), a tree connecting the sensors to the sink, such that the hop count from each sensor to the sink is no more than, say 5, the packet discard probability on each link is no more than 2.08%, and the mean delay on each link is no more than 20 msec (these single hop QoS requirements translate to an end-to-end delivery probability of 90%, and an end-to-end mean delay of 100 msec). In addition, among trees that meet these requirements, the resulting tree should achieve a large throughput region. The following are possible approaches for addressing such a problem.

Via exhaustive search using simulation or an accurate performance analysis tool: One naive way of solving the above mentioned network design problem is to consider all possible candidate tree topologies, and simulate each of them for a wide range of arrival rates to obtain their QoS respecting throughput regions, and choose the one with the largest throughput region. This method is clearly inefficient as simulation of each topology takes significant amount of time, and there could be exponentially many candidate trees (see Figure 1). An alternative approach is to replace the simulation step with a network analysis tool (such as the one proposed in [3] for IEEE 802.15.4 CSMA/CA networks) which is considerably faster compared to simulations; however, one still requires to evaluate an exponential number of candidate trees for a wide range of arrival rates, and hence the method is still inefficient.

Via a characterization of the QoS respecting throughput region: A more efficient way of solving the network design problem would be to obtain an exact analytical characterization of the QoS respecting throughput region of a tree network under IEEE 802.15.4 CSMA/CA *in terms of the topological properties of the network*, and then *derive network design rules* from that characterization to maximize the throughput region. The difficulty with this approach is that for practical CSMA/CA protocols such as IEEE 802.15.4, obtaining an explicit exact characterization of the

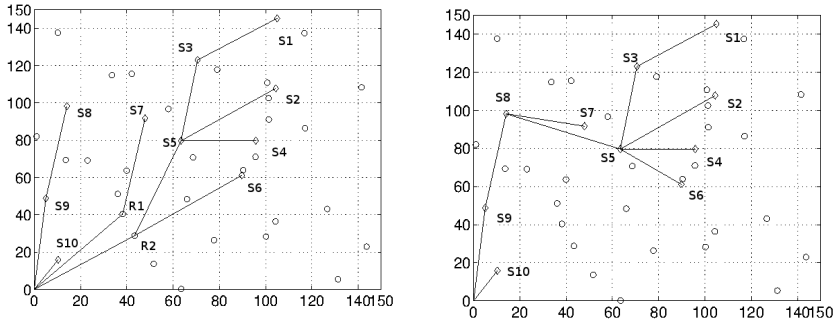

Figure 2: Two competing tree topologies obtained from the network graph in Figure 1. Left panel: a shortest path tree connecting the sources to the BS. Note that it uses two relays, namely R1 and R2. Right panel: a tree obtained using an approximation algorithm for a certain Steiner graph design problem (see the SPTiRP algorithm [1]) to connect the sources to the sink. Note that it uses no relays, but has a higher total hop count compared to the shortest path tree.

QoS respecting throughput region in terms of topological properties is notoriously hard. See Section 1.1 for more details. Therefore, some approximate methodology is in order.

Our strategy: Our approach in solving this problem is two-fold:

1. Obtain an *explicit* approximate inner bound to the QoS respecting throughput region of a tree network in terms of the topological properties of the network, and parameters of the CSMA/CA protocol.
2. Obtain a tree that maximizes this approximate inner bound.

Such an endeavour requires performance models of general multihop wireless networks under the CSMA/CA MAC, and the derivation of design criteria from such models. In this paper, we utilize our simplification of a detailed fixed point based analysis of a multi-hop tree network operating under IEEE 802.15.4 unslotted CSMA/CA [4], provided by Srivastava et al. [3], to develop certain explicit design criteria for QoS respecting networks.

As will be explained in a later section (see Section 6), it turns out that for default protocol parameters of IEEE 802.15.4 CSMA/CA, and for a wide range of QoS targets, the resulting solution is surprisingly simple: connect each sensor to the sink using a shortest path (in terms of hop count). Although this criterion is based on an approximate inner bound to the QoS respecting throughput region, we will see in our numerical experiments that this actually achieves larger throughput than a wide range of competing topologies.

Continuing the example of Figure 1, Figure 2 demonstrates two different tree topologies connecting the sensors to the sink, that are both subgraphs of the example network graph of Figure 1. The left panel shows a shortest path tree connecting the sources to the BS; this tree requires two relays. The right panel depicts a tree obtained using the SPTiRP algorithm proposed in [1] for construction of hop constrained Steiner trees with a small number of relays. In the context of this example, our results in this paper provide

i. explicit formulas for inner bounding the set of arrival rates that can be carried by either of these two topologies, while respecting the QoS objectives, and

ii. a basis for asserting that, for equal arrival rates from all sources, the shortest path tree topology in Figure 2 will achieve the larger QoS respecting arrival rate.

Indeed, for equal arrival rates from all the sensors, it turns out (by brute force search over a wide range of arrival rates using the network analysis method presented in [3] for IEEE 802.15.4 CSMA/CA) that the shortest path tree can handle up to 5 packets/sec from each source, whereas the other tree topology in Figure 2 can handle 3.5 packets/sec from each source. The corresponding values from our explicit inner bound formulas are obtained as 3.511 packets/sec and 2.605 packets/sec respectively. See Section 6 for details.

1.1. Related work

Most of the previous work on network design focuses on the "lone-packet model," or a TDMA like MAC, where there is no contention in the network; see, for example, [5, 1, 6], and the references therein. On the other hand, most work on network performance modeling focuses on estimating some measure of network performance under some simplified form of CSMA/CA MAC protocol for a *given* arrival rate vector, and a *given* network topology; see, for example, [7, 8] and the references therein. This kind of work usually involves capturing the complex interaction (due to contention) among the nodes in the network via a set of fixed point equations, and then solving these equations using an iterative scheme to obtain the quantities of interest (see [9, 10] for example). For practical MAC protocols such as IEEE 802.11 and IEEE 802.15.4, these fixed point based schemes are too involved to gather any insight on the general dependence of the network performance on the arrival rates and network topology; see, for example, [11, 12, 7]. The only papers (see [13, 14, 15]) that provide some insight on the topology dependence of the network performance do so for simplified network model and/or simplified MAC protocols that are not implemented in practice. In particular, Marbach et al. [13] provide an approximate inner bound on the stability region of a multi-hop network for a simplified CSMA/CA MAC, and Bordenave et al. [14] provide an approximate characterization of the network stability region for slotted ALOHA; however, neither work considers any QoS objective. Srinivasa and Haenggi [15] consider an infinite network where the sources nodes as well as the relay nodes are distributed according to a homogeneous Poisson point process, and analyze the throughput and end-to-end delay of a typical flow in such a network under ALOHA, and a simplified version of CSMA. They provide system design insigts such as the optimal density of source nodes, and the optimal hop count in a typical flow so as to maximize the spatial throughput density; however, their results cannot be applied in practice since practical networks are of finite size, and they do not consider any practical MAC protocol such as IEEE 802.15.4 or IEEE 802.11 CSMA/CA.

Another line of work studies the problem of joint rate control, routing and scheduling ([16, 17], and references therein) for throughput utility optimization in a given network graph. The scheduling algorithm proposed in [16] is *centralized*, and therefore, hard to implement in practice. In [17], the authors propose a distributed rate control and scheduling algorithm that is guaranteed to achieve at least half the optimal throughput region of a given network. However, none of these papers consider any QoS objective. There is related work that focuses on developing *queue length aware* CSMA/CA type distributed algorithms that can achieve the optimal throughput region, or some guaranteed fraction thereof, of a given network, while also yielding low delay [2]; see [18] and the references therein for a detailed account of the progress in this line of research. However, these queue length based distributed algorithms are

[2]Note that these scheduling algorithms essentially allow infinite number of packet retransmissions to ensure 100% end-to-end delivery

not implemented in any commercially available CSMA/CA (e.g., IEEE 802.11, IEEE 802.15.4). Therefore, we shall not pursue this line of work any further in this paper.

Our current work is *aimed as a first step towards bridging the gap between network performance modeling, and network design for a practical CSMA/CA MAC*. In particular, we are interested in deriving, from network performance models, insights on how the network performance is affected by the topology and the arrival rate vector, and then convert that insight into useful criteria for network design.

1.2. Outline of the paper

In Section 2, we describe the network model, the QoS objectives we consider in this paper, and define certain throughput regions; we then provide a summary of our contributions in the paper. Section 3 briefly describes the CSMA/CA analysis in [3], and develops a set of simplified fixed point equations starting from that analysis. In Sections 4 and 5, we use the simplified fixed point equations to derive an explicit approximate inner bound to the QoS aware throughput region of a tree network. Section 6 discusses how we can use the approximate criteria to derive a simple network design rule for a certain special case. Detailed numerical results are provided in Section 7, and we conclude in Section 8. For lack of space, some of the proofs have been provided in a technical report [2].

2. The Model, some Notation, and a Summary of the Contributions of this Paper

In this section we describe the network model, the QoS objective, some notation, and then we define certain QoS respecting throughput regions. This then permits us to provide an overview of our contributions, before we actually get into the details of the derivations, and formal results.

2.1. Network model, QoS objectives, and throughput regions

2.1.1. Network model

In this paper we focus on developing criteria for the design of tree topologies with bounded path lengths.

We consider a tree network $T = (V, E_T)$ spanning a set of sensor nodes (henceforth, called "sources"), Q (including the base station (BS)), with $|Q| = m + 1$, and a set of relays R_T such that $V = Q \cup R_T$. We assume that the edges in E_T are such that the packet error probability on any edge (for fixed packet lengths, non-adaptive modulation, fixed bit rates, and fixed transmit powers) is no more than a target value, l; the set of relays R_T may be needed to limit link lengths in order to achieve such a bound on packet error probabilities. We assume that the source-sink path lengths in T obey a given hop constraint, $h_{\max}$. As explained in [2], the choice of such a hop constraint may be affected by several factors, including the RF propagation in the given environment, and the physical characteristics of the mote hardware. In this work, we shall not concern ourselves with details of the particular choice of $h_{\max}$. We further assume that the nodes use IEEE 802.15.4 CSMA/CA for medium access. Moreover, all the nodes are assumed to be in the carrier sense range of one another. We shall refer to this assumption as the *No Hidden Nodes (NH)* assumption. For a discussion of why such an assumption may not be too restrictive, see [2].

2.1.2. QoS objectives

In order to design multi-hop networks that provide QoS, or even to route connections over such networks, given the intractability of analysis of multi-hop networks (particularly, CSMA/CA wireless networks), it has been the practice to adopt the approach of splitting the QoS over the hops along which a flow is routed (see, for example, [19, Section 5.10.1]). In this paper we adopt the approach that the end-to-end QoS objectives are *split equally* over the links on each path. That is, to meet the target end-to-end delivery probability objective p_{del}, we require that the packet discard probability on each link is no more than $\overline{\delta} =: 1 - \exp\left(\frac{\ln p_{\text{del}}}{h_{\max}}\right)$. Similarly, to meet the target end-to-end mean delay objective $d_{\max}$, we require that the mean delay on each link is no more than $\overline{d} =: \frac{d_{\max}}{h_{\max}}$. With the values of $h_{\max}$, p_{del}, $d_{\max}$ being given, we shall assume in the rest of the paper that we are given a target single-hop discard probability, $\overline{\delta}$, and a target single-hop mean delay, $\overline{d}$.

2.1.3. Throughput regions

Suppose source k generates traffic at rate λ_k packets/sec, $k = 1, \ldots, m$, according to some ergodic point process. The throughput region of a given tree network, assuming that the nodes in the network use CSMA/CA for medium access, is defined as

$\Lambda(T) = \{\underline{\lambda} = \{\lambda_k\}_{k=1}^m$: the network is *stable*$\}$

Informally speaking, the network is said to be stable when the queue lengths do not grow unbounded with time.[3] Note, however, that this notion of throughput region does not consider any QoS objective.

With our QoS splitting assumptions stated earlier, given a tree network T, and assuming the nodes in the network use CSMA/CA for medium access, we define

$\Lambda_{\overline{\delta}}(T) = \{\underline{\lambda}$: Under arrival rates $\underline{\lambda}$, the discard probability on each link in the tree T is bounded by $\overline{\delta}\}$

$\Lambda_{\overline{d}}(T) = \{\underline{\lambda}$: Under arrival rates $\underline{\lambda}$, the mean delay on each link in the tree T is bounded by $\overline{d}\}$

$\Lambda_{\overline{\delta},\overline{d}}(T) = \Lambda_{\overline{\delta}}(T) \cap \Lambda_{\overline{d}}(T)$

Note that $\Lambda_{\overline{\delta},\overline{d}} \subset \Lambda$, for otherwise, at least one queue length would grow unbounded, and the mean delay constraint would not be met.

For a tree T with arrival rates $\lambda_k(packets/sec), 1 \leq k \leq m$, at the sources, we define

$\nu_i(\underline{\lambda}, T)$: The packet rate into node i, if no packets are discarded in any node.

$h_k(T)$: The hop count on the path from source k to the sink in tree T.

For a given tree T, we then define the following throughput regions in terms of (i) a detailed fixed point analysis provided in [3], (ii) a simplified version of this fixed point analysis that we provide in this paper, and (iii) numbers $B(\overline{\delta})$ and $B'(\overline{\delta}, \overline{d})$ for which we will provide explicit formulas in terms of the parameters of the CSMA/CA protocol.

[3] See [20] for different notions of stability.

$\hat{\Lambda}_{\overline{\delta}}(T) = \{\underline{\lambda}$: Under arrival rates $\underline{\lambda}$, the discard probability on each link is bounded by $\overline{\delta}$, *according to the detailed analysis*[4] presented in [3]$\}$

$\hat{\Lambda}_{\overline{d}}(T) = \{\underline{\lambda}$: Under arrival rates $\underline{\lambda}$, the mean delay on each link is bounded by $\overline{d}$, *according to the detailed analysis* presented in [3]$\}$

$\hat{\Lambda}_{\overline{d},\overline{\delta}}(T) = \hat{\Lambda}_{\overline{d}}(T) \cap \hat{\Lambda}_{\overline{\delta}}(T)$

$\hat{\hat{\Lambda}}_{\overline{\delta}}(T) = \{\underline{\lambda}$: Under arrival rates $\underline{\lambda}$, the discard probability on each link is bounded by $\overline{\delta}$, *according to the simplified analysis* presented in Section 3.3$\}$

$\hat{\hat{\Lambda}}_{\overline{d}}(T) = \{\underline{\lambda}$: Under arrival rates $\underline{\lambda}$, the mean delay on each link is bounded by $\overline{d}$, *according to the simplified analysis* presented in Section 3.3$\}$

$\hat{\hat{\Lambda}}_{\overline{d},\overline{\delta}}(T) = \hat{\hat{\Lambda}}_{\overline{d}}(T) \cap \hat{\hat{\Lambda}}_{\overline{\delta}}(T)$

$\tilde{\Lambda}_{\overline{\delta}}(T) = \{\underline{\lambda} : \sum_{k=1}^{m} \lambda_k h_k(T) < B(\overline{\delta})\}$

$\tilde{\Lambda}_{\overline{d},\overline{\delta}}(T) = \{\underline{\lambda} : \sum_{k=1}^{m} \lambda_k h_k(T) < B(\overline{\delta})$ and $\max_{1\le i\le N} \nu_i(\underline{\lambda}, T) \le B'(\overline{\delta}, \overline{d})\}$

2.2. Contributions in this paper

With the above definitions, the main contributions of this paper are summarized as follows:

1. For the regime where packet discard probability is small, we obtain a simplified set of fixed point equations in Section 3.3. Unlike [3], *we are able to show the uniqueness of the fixed point of our simplified equations* in Section 3.4.
2. Using the simplified fixed point analysis, we provide expressions for $B(\overline{\delta})$ and $B'(\overline{\delta}, \overline{d})$ such that the following set relationships hold:

$$\tilde{\Lambda}_{\overline{d},\overline{\delta}}(T) \overset{1}{\subset} \hat{\hat{\Lambda}}_{\overline{d},\overline{\delta}}(T) \overset{2}{\approx} \hat{\Lambda}_{\overline{d},\overline{\delta}}(T)$$

   The set inequality 1 has been established in Sections 4 and 5 (see Theorems 1 and 2), where, in the process, we provide expressions for the functions $B(\overline{\delta})$, and $B'(\overline{\delta}, \overline{d})$. The "tightness" of the set inequality 1 has been evaluated through numerical experiments (see Section 7.2.2, and Table 5 in Section 7.3.2; also see Section VI-B3 in [2]). Approximation 2 has been verified through extensive numerical experiments in Section 7.2.1 for the regime where our simplified fixed point equations have a unique solution.

   These results are related to the throughput region of the original system, $\Lambda_{\overline{\delta},\overline{d}}(T)$, through the following approximation which was shown to be very accurate (well within 10% in the regime where packet discard probability on a link is about the same as the PER on the link) in [3] by extensive comparison against simulations:

$$\hat{\Lambda}_{\overline{d},\overline{\delta}}(T) \approx \Lambda_{\overline{\delta},\overline{d}}(T)$$

[4] This means that if we analyze the tree T under the given arrival rate vector $\underline{\lambda}$ using the detailed analysis, then the QoS values obtained from the analysis satisfy the target requirements.

Remark: It follows from the above set relationships that the explicitly defined set $\tilde{\Lambda}_{\overline{d},\overline{\delta}}(T)$ can be taken as an *approximate inner bound* to the original throughput region, $\Lambda_{\overline{\delta},\overline{d}}(T)$. Furthermore, our numerical experiments suggest that $\tilde{\Lambda}_{\overline{d},\overline{\delta}}(T)$ captures a significant part of the throughput region $\hat{\Lambda}_{\overline{d},\overline{\delta}}(T)$ (which, in turn, is a good approximation for $\Lambda_{\overline{\delta},\overline{d}}(T)$). In particular, when the QoS targets are in the range $\overline{\delta} \geq 0.0208$, and $\overline{d} \geq 20$ msec, for the tested network topologies, it follows from our approximate inner bound that an arrival rate of at least 2-3 packets/sec from each source can be handled without violating QoS (see Table 5 in Section 7, and the discussion thereafter). This arrival rate is more than enough for many sensor networking applications including those of industrial telemetry, and non-critical monitoring and control applications [21, 22].

3. Finally, for the special case of equal arrival rates at all the sources, default backoff parameters of IEEE 802.15.4 CSMA/CA, and a range of target values $\overline{\delta}$ and $\overline{d}$, we have shown in Section 6 that

$$\tilde{\Lambda}_{\overline{\delta}}(T) = \tilde{\Lambda}_{\overline{d},\overline{\delta}}(T) \tag{1}$$

Furthermore, let us define, for any tree T,

$$\tilde{\lambda}(T) =: \max_{\lambda : \lambda \mathbf{1} \in \tilde{\Lambda}_{\overline{d},\overline{\delta}}(T)} \lambda$$

where, $\mathbf{1}$ is the vector of all 1's having the same length as the number of sources.
Let T^* be *any shortest path tree spanning the sources and rooted at the sink*. Then, for any other tree T spanning the sources and rooted at the sink, we argue in Section 6 that

$$\tilde{\lambda}(T) \leq \tilde{\lambda}(T^*) \tag{2}$$

3. Modeling CSMA/CA for a Network with No Hidden Nodes

In this section we first briefly review the IEEE 802.15.4 CSMA/CA mechanisms, then we describe the overall modeling approach used by Srivastava et al. in [7] and [3]. This modeling approach yields a system of fixed point equations from which we derive a set of very simple fixed point equations on which the work in this paper is based.

3.1. The beaconless IEEE 802.15.4 CSMA/CA protocol

We provide a brief sketch. When a node has data to send, it initiates a random back-off [4] at the end of which it performs a CCA (*Clear Channel Assessment*) to determine whether the channel is idle. We note that, unlike the IEEE 802.11 CSMA/CA, the back-off timer of a node is not "frozen" during the transmissions of other nodes. If the CCA succeeds, the node does a *Rx-to-Tx turnaround*, which is 12 symbol times, and starts transmitting on the channel. CCA failure starts a new back-off process with the back-off exponent raised by one. After a prespecified maximum number of successive CCA failures for the same packet, the packet is discarded at the MAC layer. Upon successful packet reception, the receiver sends a fixed size ACK packet. When a transmitted packet collides or is corrupted by the PHY

layer noise, the ACK packet is not generated, which is interpreted by the transmitter as failure in delivery. The node retransmits the same packet for a prespecified maximum number of times before discarding it at the MAC layer.

3.2. The overall modeling approach in [7, 3]

Although there has been considerable research on analytical modeling of CSMA/CA, the work reported in [7], [3], in the context of beacon-less IEEE 802.15.4 CSMA/CA, appears to be the most comprehensive (capturing aspects such as multi-hopping, hop-by-hop queueing, presence of hidden terminals, etc.), and also very accurate. For ease of reference, we briefly describe the modeling philosophy of their analysis here.

In [7, 3], akin to the approach in [9] and [10], a "decoupling" approximation is made, whereby each node is modeled separately, incorporating the influence of the other nodes in the network by their average statistics, and as if these nodes were independent of the tagged node. In the literature, such an approach has also been called a "mean field approximation," and formal justification has been provided in, for example, [14].

Modeling the activity of a tagged node, say i: All packets entering node i are assumed to have the same fixed length, and hence the same fixed transmission time over the medium (denoted by T_{tx}). In a network with no hidden nodes, the channel activity perceived by node i is due to all the other nodes in the network. Each node alternates between periods during which its transmitter queue is empty and those during which the queue is non-empty. During periods in which its transmitter queue is non-empty, when the node is not transmitting it is performing repeated backoffs for the head-of-the-line (HOL) packet in its queue. Each backoff ends in a CCA attempt. Figure 3 is a depiction of this alternation in node behavior *during the periods when its queue is nonempty*. We employ the decoupling approximation to analyse this process.

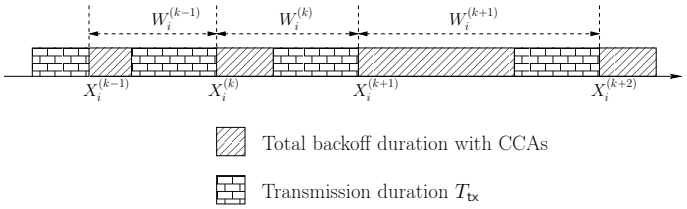

Figure 3: (Taken from [3]) The alternating (contention-transmission) process obtained by observing the process at a node i after removing all the idle time periods at Node i. The transmission completion epochs are denoted by $\{X_i^{(k)}\}$ and the contention-transmission cycle lengths by $\{W_i^{(k)}\}$.

Focusing on durations during which Node i's queue is nonempty (see Figure 3), consider the completion of a transmission by Node i; this could have been a success or a collision. We note that packet collisions can occur even in the absence of hidden nodes, since transmissions from two transmitters placed within the CS range of each other can overlap (known as **Simultaneous Channel Sensing**), as depicted in Figure 4.

Due to the small propagation delay, and the no hidden nodes assumption, we neglect the up to 12 additional symbol durations for which other simultaneous transmissions could last. After the completion of its transmission, Node i contends for the channel by executing successive backoffs; the nodes $j \neq i$ either have non-empty queues and are also contending, or have empty queues and are not contending. With these observations in mind, the CCA attempt process at Node i *conditioned on being in backoff periods* is modeled as a Poisson process of rate β_i. For each node

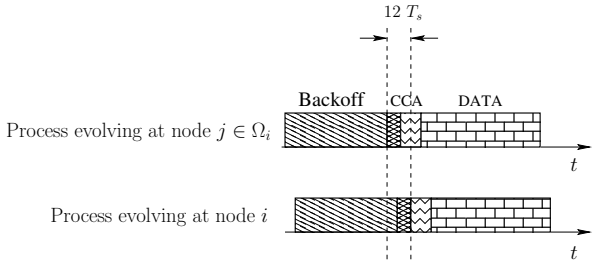

Figure 4: (Taken from [3]) Node j finishes its backoff, performs a CCA, finds the channel idle and starts transmitting the DATA packet. Node i finishes its backoff anywhere in the shown 12 T_s duration and as there is no other ongoing transmission in the network, its CCA succeeds and it enters the transmission duration. As a result, the DATA packets may collide at receiver of i or that of j.

$j \neq i$, the CCA attempt process, conditioned on j's queue being non-empty *and* being in backoff, or being empty, is modeled by an independent Poisson process with rate $\overline{\tau}_j^{(i)}$, $j \neq i$. This is the rate of attempts of Node j as perceived by Node i during Node i's back-off periods.

Now let us return to the process depicted in Figure 3, i.e., the alternating contention and transmission periods of Node i when its queue is nonempty. As a result of the assumption of independent Poisson attempt processes at the nodes, it can be observed that the instants $X_i^{(k)}$ are renewal instants, and the intervals $W_i^{(k)}$ form an i.i.d.[5] sequence.

With the above observations and definitions, the detailed evolution of the attempt processes at the nodes can be analyzed using renewal theoretic arguments, thus leading to a set of fixed point equations involving quantities such as the collision probability, the CCA failure probability, the rates of CCA attempts, the packet discard probability at a node, queue non-empty probability of a node, and the probability that a node is in back-off conditioned on its queue being non-empty. The resulting fixed point equations, for the NH case, are shown in [2, Section II-B2].

The analysis of packet delay between a source node and the sink node utilizes the approximation techniques in Whitt's Queueing Network Analyzer (QNA, [23]). The arrival processes at the source nodes are modeled as independent Poisson processes.[6] Each node is modeled by a GI/GI/1 queue. Using the solution to the fixed point equations obtained earlier, the first two moments of the service time at each queue can be computed. The arrival and departure processes of the nodes are approximated by renewal processes, whose first two moments are computed recursively, starting from the leaf nodes, and using the solution to the fixed point equations obtained earlier. Given the first two moments of the interarrival time and of the service time, QNA uses a standard GI/GI/1 mean delay approximation for the mean delay at a queue. In this manner, starting with the model of the input processes at the source nodes, the end-to-end mean delay can be approximated.

In [3], the authors find that the analysis is accurate to within 10% in the regime where the discard probability on a link is about the same as the PER on that link.

It is evident from the complex structure of the fixed point equations displayed in [2] that even for the no hidden nodes case, it is difficult to use this analysis to extract insight about the relation between network topology and the

[5]Independently and identically distributed

[6]We note that the methodology does not rely on this Poisson arrivals assumption. Other renewal arrival processes can be assumed, including periodic arrivals.

QoS measures. We therefore, in the next section, resort to simplifying these detailed equations in a certain regime of network operation.

3.3. Simplified fixed point equations in the low discard regime

Our point of departure from the analysis in [3] is to show that, in the low discard regime[7], the fixed point equations can be substantially simplified. We have obtained this simplification by introducing the following approximations that are approximately valid in the low discard regime.

(A1) The discard probability at any node i, $\delta_i \approx 0$ so that the total arrival rate into node j is $\nu_j = \sum_{k=1}^{m} z_{k,j}\lambda_k$, where $z_{k,j} = 1$ iff node j is in the path of source k, and $z_{k,j} = 0$ otherwise.

(A2) The probability, r_i, that the head-of-line (HOL) packet at node i encounters a transmission failure is very small, i.e., $r_i \ll 1$.

(A3) The fraction of time, q_i, that the queue of node i is non-empty is very small, i.e., $q_i \ll 1$.

(A4) The probability, c_i, that node i finishes its backoff within 12 symbol times after another node has finished backoff is negligibly small, i.e., $c_i \approx 0$.

(A5) The probability, γ_i, that a transmitted packet from node i encounters a collision or link error is very small, i.e., $\gamma_i \ll 1$, so that $(1 - \gamma_i) \approx 1$.

With these approximations, it easily turns out (by simple substitution of the approximations) that the detailed fixed point equations in [3] simplify to the following vector fixed point equations (see [2] for details):

$$\overline{\tau}_{-i} = \sum_{j \neq i} \left(\sum_{k=1}^{m} z_{k,j}\lambda_k \right) (1 + \alpha_j + \ldots + \alpha_j^{n_c - 1}) \; \forall i = 1, \ldots, N \tag{3}$$

$$\alpha_i = \frac{T_{\mathsf{tx}}\overline{\tau}_{-i}}{1 + T_{\mathsf{tx}}\overline{\tau}_{-i}} \; \forall i = 1, \ldots, N \tag{4}$$

where, $\overline{\tau}_{-i}$ is the total CCA attempt rate *seen* by node i, and α_i is the CCA failure probability at node i.

Although these equations have been derived by introducing the above approximations in the detailed equations of [3], it is easy to provide a direct intuition for them as follows.

Consider the term corresponding to node j in the summation in (3). Note that the first factor in this term is the total arrival rate into a node j, and the second factor is the mean number of CCA attempts of a packet at node j. Thus, each term inside the summation is the total CCA attempt rate due to a node. Hence the summation (which does not include node i) is indeed the total CCA attempt rate *seen* by node i. Here, of course, we are invoking the NH property of the network.

[7] Note that a single-hop discard probability of even 3% results in an end-to-end delivery probability less than 90% on a path with 4 or more hops; hence, for most practical purposes, we would be interested in operating the network in the low discard regime.

Also, let us define $N_i^{CCA}(t)$ and $N_i^{CCAf}(t)$ to be the number of CCA attempts and number of CCA failures respectively at node i up to time t. Then, $\alpha_i = \lim_{t\to\infty} \frac{N_i^{CCAf}(t)}{N_i^{CCA}(t)}$, which by using the renewal model discussed in Section 3.2, and elementary ergodic results, gives

$$\alpha_i = \frac{N_i^{CCAf}}{N_i^{CCA}} \tag{5}$$

where N_i^{CCA} is the mean number of total CCA attempts by node i in a renewal cycle, and N_i^{CCAf} is the mean number of failed CCA attempts by node i in a renewal cycle.

Note that when node i's backoff finishes first among all contending nodes (this happens with probability $\frac{\beta_i}{\beta_i+\overline{\tau}_{-i}}$), its first CCA succeeds, and the cycle ends after node i's transmission. When some other contending node's backoff finishes first (this happens with probability $\frac{\overline{\tau}_{-i}}{\beta_i+\overline{\tau}_{-i}}$), that node starts transmitting on the medium, and node i continues to perform CCAs at rate β_i for the entire transmission duration T_{tx}, i.e., a total of $\beta_i T_{\text{tx}}$ CCAs, all of which fail (note that we are using (A4) in making this assertion); at the end of the transmission duration, all the nodes again enter contention, and the cycle continues. Using these observations, N_i^{CCA} can be written recursively as

$$N_i^{CCA} = \frac{\beta_i}{\beta_i + \overline{\tau}_{-i}} \cdot 1 + \frac{\overline{\tau}_{-i}}{\beta_i + \overline{\tau}_{-i}} (\beta_i T_{\text{tx}} + N_i^{CCA})$$

This, after simplification, yields,

$$N_i^{CCA} = 1 + \overline{\tau}_{-i} T_{\text{tx}}$$

Using similar arguments, N_i^{CCAf} can be written recursively as

$$N_i^{CCAf} = \frac{\beta_i}{\beta_i + \overline{\tau}_{-i}} \cdot 0 + \frac{\overline{\tau}_{-i}}{\beta_i + \overline{\tau}_{-i}} (\beta_i T_{\text{tx}} + N_i^{CCAf})$$

This, after simplification, yields,

$$N_i^{CCAf} = \overline{\tau}_{-i} T_{\text{tx}}$$

Finally, plugging these back into (5), we have

$$\alpha_i = \frac{T_{\text{tx}} \overline{\tau}_{-i}}{1 + T_{\text{tx}} \overline{\tau}_{-i}}$$

We now write down certain other quantities of interest in terms of the fixed point variables. Using (A4), the probability of a packet collision (or, equivalently, the probability of simultaneous channel sensing) is easily seen to be (recall the modeling philosophy from Section 3.2) $(1 - \exp(-12\overline{\tau}_{-i}))$. Hence, the transmission failure probability, γ_i at node i can

be written as

$$\gamma_i = l + (1 - l)(1 - \exp(-12\overline{\tau}_{-i})) \tag{6}$$

where we have assumed the worst case PER l on a link.

The packet discard probability at node i, denoted δ_i, is given by

$$\delta_i = \alpha_i^{n_c}(1 + r_i + r_i^2 + \ldots + r_i^{n_t-1}) + r_i^{n_t} \tag{7}$$

where, $r_i = \gamma_i(1 - \alpha_i^{n_c})$ is the probability that the HOL packet at node i was transmitted, and it encountered a transmission failure (either due to collision or due to link error). n_c and n_t denote respectively, the maximum allowed number of successive CCA failures, and the maximum allowed number of transmission failures after which the packet is discarded.

Finally, the CCA attempt rate, β_i, conditioned on being in back-off periods, can be written as

$$\beta_i = \frac{1 + \alpha_i + \alpha_i^2 + \ldots + \alpha_i^{n_c-1}}{\overline{B}_i} \tag{8}$$

This can be interpreted as a consequence of the Renewal Reward Theorem (RRT; see, for example, [24]), where the numerator is the mean number of CCA attempts for the HOL packet at node i, and the denominator, $\overline{B}_i$, is the mean time spent in backoff by the HOL packet at node i. For default back-off parameters of IEEE 802.15.4 CSMA/CA,

$$\overline{B}_i = 78 + 158\alpha_i + 318(\alpha_i^2 + \alpha_i^3 + \cdots + \alpha_i^{n_c-1}) \tag{9}$$

It is easy to see (using Lemma 5.1 in [25]) that β_i is non-increasing in α_i.

Suppose L_j is the set of nodes on the path from source j to the sink. Then, assuming packet discards are independent across nodes, *the end-to-end delivery probability* of source j is given by $\prod_{i \in L_j}(1 - \delta_i)$, where δ_i is the packet discard probability at node i as defined earlier.

Simplifications for delay approximation

We have listed the detailed equations for delay approximation in Section II-B2 of [2]. We write down here, the simplifications we obtain from those equations under approximations (A1)-(A5) (see [2] for details).

The end-to-end mean packet delay for a source node j, provided that the set of nodes along the path from this node to the BS is L_j, is given by

$$\Delta_j \quad = \quad \sum_{i \in L_j} \overline{\Delta}_i \tag{10}$$

where, $\overline{\Delta}_i$ is the mean sojourn time at a node i, and is given by (also see Eqn. 19 in [2], and the discussion leading to Eqn. 24 in [2])

$$\overline{\Delta}_i = \frac{\rho_i \mathbb{E}(S_i)(1 + c_{S_i}^2)}{2(1-\rho_i)} + \mathbb{E}(S_i) \tag{11}$$

Here, $\rho_i = \nu_i \mathbb{E}(S_i)$ denotes the traffic load at node i with $\nu_i = \sum_{k=1}^{m} z_{k,i}\lambda_k$ being the total arrival rate into node i, S_i denotes the service time at node i, and $c_{S_i}^2 = \frac{Var(S_i)}{\mathbb{E}^2(S_i)}$ is the squared coefficient of variance of service time at node i.

Note that the above expression is precisely the Pollaczek-Khintchine formula (see, for example, [24]) for the mean delay of an M/G/1 queue. Thus, in the low discard regime, the delay approximation (see Eqn. 19 in [2]) reduces to modeling each node in the network by an M/G/1 queue.

Furthermore, the MGF $M_{S_i}(z)$ of S_i can be expressed as (see [3]),

$$M_{S_i}(z) \quad = \quad \frac{\beta_i(1-\alpha_i)(1-\gamma_i)e^{-zT_{\text{tx}}}}{z + \beta_i(1-\alpha_i)(1-\gamma_i e^{-zT_{\text{tx}}})}.$$

Starting with this MGF, and taking derivative w.r.t z, straightforward calculations yield,

$$\mathbb{E}(S_i) = -\frac{d}{dz}M_{S_i}(z)\Big|_{z=0} = \frac{1 + \beta_i(1-\alpha_i)T_{\text{tx}}}{\beta_i(1-\alpha_i)(1-\gamma_i)} \tag{12}$$

where we recall from Section 3.2 that β_i is the mean CCA attempt rate of node i conditioned on being in backoff periods. β_i is a function of α_i and the protocol parameters (see (8)).

Similarly, by straightforward calculations,

$$\begin{aligned}\mathbb{E}(S_i^2) = \frac{d^2}{dz^2}M_{S_i}(z)\Big|_{z=0} &= T_{\text{tx}}^2 + \frac{2T_{\text{tx}}}{\beta_i(1-\alpha_i)(1-\gamma_i)} + \frac{3\beta_i(1-\alpha_i)\gamma_i T_{\text{tx}}^2}{\beta_i(1-\alpha_i)(1-\gamma_i)} \\ &+ \frac{2(1+\beta_i(1-\alpha_i)\gamma_i T_{\text{tx}})^2}{(\beta_i(1-\alpha_i)(1-\gamma_i))^2}\end{aligned} \tag{13}$$

Finally, after some algebraic manipulations, we have

$$c_{S_i}^2 = \frac{Var(S_i)}{\mathbb{E}^2(S_i)} = \gamma_i + \frac{1-\gamma_i}{(1+\beta_i(1-\alpha_i)T_{\text{tx}})^2} \approx \gamma_i + \frac{1}{(1+\beta_i(1-\alpha_i)T_{\text{tx}})^2} \tag{14}$$

where, in Eqn. (14), we have used (A5).

Remark: In our numerical experiments with default backoff parameters, the above simplifications yield delay values that are accurate to within 6% w.r.t the delay values obtained from the detailed analysis, which themselves were accurate to well within 10%.

In what follows, we shall use this simplified fixed point analysis to obtain sufficient conditions for the membership of $\hat{\Lambda}_{\overline{\delta}}$ and $\hat{\Lambda}_{\overline{d}}$.

We start by establishing a condition for the uniqueness of the solution to the simplified vector fixed point equations (3) and (4).

3.4. Existence and uniqueness of the simplified vector fixed point

Let us define $\alpha_{\max} =: \overline{\delta}^{1/n_c}$, and $a =: \frac{\alpha_{\max}}{T_{tx}(1-\alpha_{\max})}$, where $\overline{\delta}$ is the target discard probability (at a node) as defined earlier. Observe from Equation (4) that $\alpha_i \leq \alpha_{\max} \Leftrightarrow \overline{\tau}_{-i} \leq a$. Moreover, note that in our regime of interest, i.e., the regime where $\max_{1\leq i\leq N} \delta_i \leq \overline{\delta}$, we have $\alpha_i \leq \alpha_{\max}$ for all $i = 1, \ldots, N$, or equivalently, $\overline{\tau}_{-i} \leq a$ for all $i = 1, \ldots, N$. Then, we have the following proposition.

Proposition 1. *If*

$$\sum_{k=1}^{m} \lambda_k h_k < \min\left\{\frac{a}{1+\alpha_{\max}+\ldots\alpha_{\max}^{n_c-1}},\ \frac{1}{T_{tx}(1+2\alpha_{\max}+\ldots+(n_c-1)\alpha_{\max}^{n_c-2})}\right\} =: B_1(\overline{\delta}) \tag{15}$$

then the simplified fixed point equations defined by (3) *and* (4) *have a unique solution* $\{\overline{\tau}_{-i}\}_{i=1}^{N}$ *in* $[0, a]^N$.

Proof. The proof proceeds by establishing that the simplified fixed point equations define a contraction mapping on $[0, a]^N$. See Appendix 9.2 for details. □

We call the regime defined by Equation (15) the *uniqueness regime*. Our numerical experiments suggest that in this regime, the simplified fixed point equations well-approximate the detailed fixed point equations (to within 10% for $\overline{\tau}_{-i}$), i.e., we have $\hat{\Lambda}_{\overline{d},\overline{\delta}} \approx \hat{\hat{\Lambda}}_{\overline{d},\overline{\delta}}$, where $\hat{\Lambda}_{\overline{d},\overline{\delta}}$ and $\hat{\hat{\Lambda}}_{\overline{d},\overline{\delta}}$ are as defined in Section 2.1.3. See Section 7 for details.

In light of above discussion, we shall focus on obtaining sufficient conditions for membership of $\hat{\hat{\Lambda}}_{\overline{\delta}}$ and $\hat{\hat{\Lambda}}_{\overline{d}}$ instead of $\hat{\Lambda}_{\overline{\delta}}$ and $\hat{\Lambda}_{\overline{d}}$.

4. Derivation of A Sufficient Condition for Membership of $\hat{\hat{\mathbf{\Lambda}}}_{\overline{\boldsymbol{\delta}}}$

In this section, we shall derive a sufficient condition for the membership of the set $\hat{\hat{\Lambda}}_{\overline{\delta}}(T)$ (defined in Section 2.1.3) for a given tree T. In other words, we shall derive the structure of the set $\tilde{\Lambda}_{\overline{\delta}}(T)$ introduced in Section 2.1.3.

4.1. A control on the maximum packet discard probability

From equation (7), we can derive the following Lemma.

Lemma 1. *For* $\alpha_i^{n_c} \leq 1/n_t$, *and* $\gamma_i^{n_t} \leq 1/n_t$, *the packet discard probability at node i,* δ_i, *is monotonically increasing in* α_i *and* γ_i, *i.e.,* $\delta_{i,1} \leq \delta_{i,2}$ *whenever* $\alpha_{i,1} \leq \alpha_{i,2}$ *and* $\gamma_{i,1} \leq \gamma_{i,2}$.

Proof. The proof proceeds by showing that $\delta_i(\alpha_i, \gamma_i)$ is increasing in each coordinate when the other coordinate is held fixed. See [2] for details. □

From the simplified fixed point equations (3), (4), and (6), we have the following lemma. Since the proof is short, we present the proof here itself.

Lemma 2. α_i *and* γ_i *are monotonically increasing in* $\overline{\tau}_{-i}$.

Proof. From (6), it is clear that γ_i is monotonically increasing in $\overline{\tau}_{-i}$. To see that α_i is monotonically increasing in $\overline{\tau}_{-i}$, observe that the derivative of the R.H.S of (4) w.r.t $\overline{\tau}_{-i}$ is non-negative. □

Combining Lemmas 1 and 2, we have

Proposition 2. *δ_i is monotonically increasing in $\overline{\tau}_{-i}$.*

It follows from Proposition 2 that to control the maximum packet discard probability, we need to control $\max_{i=1,\ldots,N} \overline{\tau}_{-i}$, i.e.,

$$\max_{i=1,\ldots,N} \delta_i \leq \overline{\delta} \Leftrightarrow \max_{i=1,\ldots,N} \overline{\tau}_{-i} \leq \tau_{\max}$$

where $\tau_{\max}$ is the upper bound on $\overline{\tau}_{-i}$ that ensures $\delta_i \leq \overline{\delta}$.

4.2. A scalar fixed point

Before proceeding further, we take a slight detour, and introduce a further simplification to the fixed point equations described in Section 3.3. We shall obtain a scalar fixed point equation which will be exploited later on to extract information about topological dependencies.

We start with the following observation from our numerical experiments with the detailed analysis (see Section 7.2.2).

Observation 1. *For all $i = 1, \ldots, N$,*

$$\overline{\tau}_{-i} \approx \overline{\tau}$$

i.e., the total attempt rate seen by a node is roughly equal for all nodes, and is approximately equal to the total attempt rate, denoted $\overline{\tau}$, in the network.

An analytical intuition behind this observation for large N is also provided in [2].

From the above observation, and (4), it follows that the CCA failure probabilities of the nodes are roughly equal, and are equal to $\alpha = \frac{T_{tx}\overline{\tau}}{1+T_{tx}\overline{\tau}}$.

Moreover, the total CCA attempt rate, $\overline{\tau}$, in the network can be computed as $\overline{\tau} = (\sum_{k=1}^{m} \lambda_k h_k)(1 + \alpha + \ldots + \alpha^{n_c-1})$, where the first factor on the R.H.S is the total packet arrival rate into the network, and the second factor is the mean number of CCA attempts due to each packet.

Thus, we have the following scalar fixed point equation in $\overline{\tau}$, the total attempt rate in the network:

$$\overline{\tau} = (\sum_{k=1}^{m} \lambda_k h_k)(1 + \alpha + \ldots + \alpha^{n_c-1}) \tag{16}$$

$$\alpha = \frac{T_{tx}\overline{\tau}}{1 + T_{tx}\overline{\tau}} \tag{17}$$

Note that (17) can also be written as $\alpha = \frac{T_{tx}}{\frac{1}{\overline{\tau}}+T_{tx}}$, which can be interpreted as the fraction of time that the medium is occupied by a packet (consequently, all CCA attempts during this time fail).

4.3. Existence and uniqueness of the scalar fixed point

Let us, as before, define $a =: \frac{\alpha_{\max}}{T_{tx}(1-\alpha_{\max})}$, where $\alpha_{\max} = \overline{\delta}^{1/n_c}$. Observe from (17) that $\alpha \leq \alpha_{\max} \Leftrightarrow \overline{\tau} \leq a$. Then, we have the following proposition.

Proposition 3. *If the condition defined by* (15) *holds, then the scalar fixed point equation defined by* (16),(17) *has a unique solution in* $[0, a]$.

Proof. The proof proceeds by showing that the scalar fixed point equation defines a contraction mapping on $[0, a]$. See Appendix 9.3 for details. □

Note that (15) ensures unique fixed point for both the vector and the scalar fixed point equations.

4.4. A tight upper bound on $\max_{1\leq i\leq N} \overline{\tau}_{-i}$

We now come back to the main thread of our discussion. Recall the scalar fixed point equations (16), (17) derived in Section 4.2. We had promised that these equations will find use in deriving topological properties that control the network performance. To this end, we start with the following proposition.

Proposition 4. *In the uniqueness regime (defined by* (15)*),*

$$\overline{\tau} \geq \max_{1\leq i\leq N} \overline{\tau}_{-i} \tag{18}$$

where $\overline{\tau}$ *is the unique solution to the scalar fixed point equations* (16),(17)*, and* $\{\overline{\tau}_{-i}\}_{i=1}^{N}$ *is the unique solution to the simplified vector fixed point equations* (3),(4).

Proof. The proof is via induction. See Appendix 9.4 for details. □

Remarks:

(a) The intuition behind the above proposition is clear. Each component of the simplified vector fixed point approximates the total attempt rate *seen* by the corresponding node in the network, which should clearly be upper bounded by the total attempt rate of all the nodes in the network, approximated by the scalar fixed point.

(b) Observation 1 (from our numerical experiments) suggests that the above upper bound on $\max_{1\leq i\leq N} \overline{\tau}_{-i}$ is tight. Further numerical experiments verifying the tightness of the bound are provided in Section VI-B3 of [2].

From Proposition 4, it follows that to ensure $\max_{1\leq i\leq N} \overline{\tau}_{-i} \leq \tau_{\max}$, it *suffices* that we ensure $\overline{\tau} \leq \tau_{\max}$, i.e., to control the maximum packet discard probability, $\max_{1\leq i\leq N} \delta_i$ (or, equivalently, $\max_{1\leq i\leq N} \overline{\tau}_{-i}$; recall Proposition 2, and the discussion thereafter), it suffices to control the approximate total attempt rate, $\overline{\tau}$. We, therefore, next investigate the dependence of $\overline{\tau}$ on the network topology and arrival rate vector to come up with a sufficient condition for the membership of $\hat{\hat{\Lambda}}_{\overline{\delta}}$.

4.5. A sufficient condition for membership of $\hat{\hat{\Lambda}}_{\overline{\delta}}$

The following proposition is an easy consequence of Part 2 of Lemma 5 stated in Appendix 9.3, and hence we omit the proof.

Proposition 5. *$\overline{\tau}$, the solution to the scalar fixed point equations* (16),(17)*, is monotonically increasing in $\sum_{k=1}^{m} \lambda_k h_k$.*

It follows from Proposition 5 that given $\overline{\delta}$ (or, equivalently, $\tau_{\max}$), there exists $B_2(\overline{\delta})$ such that $\sum_{k=1}^{m} \lambda_k h_k \leq B_2(\overline{\delta}) \Leftrightarrow \overline{\tau} \leq \tau_{\max}$. Hence, as long as the vector fixed point equations (3),(4) and the scalar fixed point equations (16),(17) have unique solutions, the following sequence of implications hold:

$$\sum_{k=1}^{m} \lambda_k h_k \leq B_2(\overline{\delta}) \Rightarrow \overline{\tau} \leq \tau_{\max} \Rightarrow \max_{1 \leq i \leq N} \overline{\tau}_{-i} \leq \tau_{\max} \Rightarrow \max_{1 \leq i \leq N} \delta_i \leq \overline{\delta}$$

However, (15) gives us a sufficient condition for a unique solution of the fixed point equations. Thus, we have the following theorem:

Theorem 1. *Let $B(\overline{\delta}) =: \min\{B_1(\overline{\delta}), B_2(\overline{\delta})\}$, where $B_1(\overline{\delta})$ is as defined in* (15)*, and $B_2(\overline{\delta})$ is as defined in the above discussion. Suppose, for a given tree network topology, an arrival rate vector $\underline{\lambda}$ satisfies*

$$\sum_{k=1}^{m} \lambda_k h_k < B(\overline{\delta}) \tag{19}$$

Then, $\underline{\lambda} \in \hat{\hat{\Lambda}}_{\overline{\delta}}$.

Note that the above theorem characterizes the set $\tilde{\Lambda}_{\overline{\delta}}(T)$ introduced in Section 2.1.3.

5. Derivation of a Sufficient Condition for the Membership of $\hat{\hat{\Lambda}}_{\overline{d},\overline{\delta}}$

In this section, we shall derive a sufficient condition for the membership of $\hat{\hat{\Lambda}}_{\overline{d},\overline{\delta}}$, thereby defining the set $\tilde{\Lambda}_{\overline{d},\overline{\delta}}(T)$ for a given tree T.

5.1. Dependence of $\mathbb{E}(S_i)$ and $c_{S_i}^2$ on $\overline{\tau}_{-i}$

We make the following claim.

Lemma 3. *$\mathbb{E}(S_i)$ and $c_{S_i}^2$ are monotonically increasing in $\overline{\tau}_{-i}$.*

Proof. See [2]. □

5.2. A bound on $\overline{\Delta}_i$

Recall from Proposition 2 that the constraint on the packet discard probability, namely $\max_{1 \leq i \leq N} \delta_i \leq \overline{\delta}$, translates to a constraint on $\overline{\tau}_{-i}$, namely $\max_{1 \leq i \leq N} \overline{\tau}_{-i} \leq \tau_{\max}$. This, together with Lemma 3, implies a bound on $\mathbb{E}(S_i)$ and on $c_{S_i}^2$, namely that, for all i, $\mathbb{E}(S_i) \leq \overline{S}$, and $c_{S_i}^2 \leq \overline{c_S^2}$. Noting that $\frac{\rho_i}{1-\rho_i}$ is monotonically increasing in ρ_i, This yields a bound on $\overline{\Delta}_i$ for fixed ν_i, namely,

$$\overline{\Delta}_i \leq \frac{\nu_i \overline{S}}{2(1 - \nu_i \overline{S})} \overline{S}(1 + \overline{c_S^2}) + \overline{S}$$

5.3. A sufficient condition for membership of $\hat{\tilde{\Lambda}}_{\overline{d},\overline{\delta}}$

In order that $\overline{\Delta}_i \leq \overline{d}$ for all i, it suffices that for all i, $\frac{\nu_i \overline{S}}{2(1-\nu_i \overline{S})}\overline{S}(1+\overline{c_S^2}) + \overline{S} \leq \overline{d}$. After some straightforward algebraic manipulations, this yields an upper bound, designated by $B'(\overline{\delta}, \overline{d})$, on ν_i for all i. Thus, we have the following theorem:

Theorem 2. *If an arrival rate vector* $\underline{\lambda} = \{\lambda_k\}_{k=1}^m$ *satisfies Equation* (19)*, and the following holds:*

$$\max_{1 \leq i \leq N} \nu_i \leq B'(\overline{\delta}, \overline{d}) \tag{20}$$

where $\nu_i = \sum_{k=1}^m z_{k,i}\lambda_i$*, and* $B'(\overline{\delta}, \overline{d})$ *is as defined in the above discussion, then,* $\underline{\lambda} \in \hat{\tilde{\Lambda}}_{\overline{d},\overline{\delta}}$.

Note that the above theorem characterizes the set $\tilde{\Lambda}_{\overline{d},\overline{\delta}}(T)$ introduced in Section 2.1.3.

From the definitions of $\tilde{\Lambda}_{\overline{\delta}}(T)$, and $\tilde{\Lambda}_{\overline{d},\overline{\delta}}(T)$, it also follows that $\tilde{\Lambda}_{\overline{\delta}}(T) \supset \tilde{\Lambda}_{\overline{d},\overline{\delta}}(T)$.

6. Special Case: Equal Arrival Rates at All Sources

In this section, we shall focus on the notion of equal throughput, i.e., the scenario where the external arrival rates at all the sources are equal, say, λ. This leads to the following interesting consequences.

1. Condition (20) reduces to $\lambda \max_{1 \leq i \leq N} m_i \leq B'$, whereas, condition (19) reduces to $\lambda \sum_{i=1}^N m_i \leq B$, where m_i is the number of sources whose paths to the sink use node i. Now, for default backoff parameters, and for $\overline{\delta} = .0208$, $\overline{d} = 20$ msec (corresponding to, for example, $p_{\text{del}} = 90\%$ and $d_{\max} = 100$ msec for $h_{\max} = 5$), it turns out that $B(\overline{\delta}) = 80.75$ packets/sec, and $B'(\overline{\delta}, \overline{d}) = 82.85$ packets/sec, i.e., $B(\overline{\delta}) < B'(\overline{\delta}, \overline{d})$ so that for all λ satisfying the discard probability objective (19), $\lambda \max_{1 \leq i \leq N} m_i \leq \lambda \sum_{i=1}^N m_i < B(\overline{\delta}) < B'(\overline{\delta}, \overline{d})$, i.e., the mean delay objective (20) is also satisified. Hence, it follows that for equal arrival rates, and default backoff parameters, $\tilde{\Lambda}_{\overline{d},\overline{\delta}} = \tilde{\Lambda}_{\overline{\delta}}$. Furthermore, it was observed that this conclusion continues to hold for a range of QoS targets such that $.015 \leq \overline{\delta} \leq 0.04$ and 20 msec $\leq \overline{d} \leq 45$ msec.
2. **A simple network design criterion:** Suppose we are given a graph $G = (V, E)$ with $V = Q \cup R$, where R is a set of *potential* locations where one can place relays, and E is the set of *admissible* edges with PER at most l. Our objective is to design a tree network spanning the sources and the BS, possibly using a few relays (placed at a subset of the potential locations), such that the resulting network meets a given hop constraint $h_{\max}$ on each source-sink path, and meets given per-hop discard probability and mean delay targets, while achieving a large throughput region.

   In light of the discussion in Item 1 above, for default backoff parameters and reasonable QoS targets, an approximate lower bound to the throughput of a given tree network topology is $\frac{B(\overline{\delta})}{\sum_{k=1}^m h_k}$ (using $\tilde{\Lambda}_{\overline{d},\overline{\delta}}$ as an approximate inner bound to $\Lambda_{\overline{\delta},\overline{d}}$; recall the set relationships from Section 2.2). This, in turn, gives a *simple criterion for approximately throughput optimal network design* for the case of equal arrival rates, namely, *obtain a tree that minimizes the total hop count from the sources to the sink,* $\sum_{k=1}^m h_k$; this is nothing but the *shortest path tree* over graph G (with hop count as cost).[8] Note that this is simply a re-wording of Equation (2) stated in Section 2.2.

[8] Note that if the hop constraint, $h_{\max}$, is feasible, the shortest path tree will also meet the hop constraint.

Observe that the same criterion holds for the notion of max min throughput (see, for example, [2] for a formal definition), since the max-min is achieved along the direction of equal arrival rates.

Further discussion of the example introduced in Figures 1 and 2: Recall the example introduced in Figures 1 and 2 in Section 1. Observe that our experimental observation there that the shortest path tree achieves a better throughput than the other topology matches with our theoretical observation in Item 2 above.

Moreover, for the given QoS requirements, and default backoff parameters, it follows from the discussion above that the shortest path tree (left panel of Figure 2) can handle an arrival rate of at least $\frac{B(\bar{\delta})}{\sum_{k=1}^{m} h_k} = \frac{80.75}{23} = 3.511$ packets/sec from each source, whereas the topology obtained from SPTiRP algorithm [1] (right panel of Figure 2) can handle an arrival rate of at least $\frac{B(\bar{\delta})}{\sum_{k=1}^{m} h_k} = \frac{80.75}{31} = 2.605$ packets/sec from each source. Note that these lower bounds are obtained using our explicit formula for the set $\tilde{\Lambda}_{\bar{d},\bar{\delta}}$ as opposed to a brute force search over all possible arrival rates, and hence are much simpler to compute.

As we shall see in our numerical experiments (Section 7), although the shortest path tree criterion is based on an approximation to $\Lambda_{\bar{\delta},\bar{d}}$, it, in fact, achieves better throughput than a wide range of competing topologies.

7. Numerical Results

7.1. The setting

We conducted all our numerical experiments using the default protocol parameters of IEEE 802.15.4 CSMA/CA. In particular, we assumed $n_c = 5$, $n_t = 4$, and default back-off parameters ([4]) in all the experiments.

We chose the worst case packet error rate (PER) on each link to be $l = 2\%$, and packet length $T = 131$ bytes[9]. The target packet discard probability, $\bar{\delta} = 0.0208$, and the target single-hop mean delay $\bar{d} = 20$ msec (which correspond, for example, to a target end-to-end delivery probability $p_{\text{del}} = 90\%$, and target end-to-end mean delay $d_{\max} = 100$ msec for a hop constraint $h_{\max} = 5$). We assumed equal arrival rates at all the sources for the experiments.

All the experiments were conducted on 5 random network topologies, each of which was generated as follows: 10 sources and 30 potential relay locations were selected uniformly at random over a 150×150 m^2 area. The sink was chosen at a corner point of the area. A Steiner tree was then formed connecting the sources to the sink, using no more than 4 relays[10], such that the hop count from each source to the sink was at most 5. The algorithm used to form this Steiner tree is a variation of the SPTiRP algorithm ([1]), and is described in the Appendix.

7.2. Model validation

7.2.1. Accuracy of the simplified vector fixed point equations

To verify the accuracy of the simplified vector fixed point equations (3) in the uniqueness regime (described by Eqn. (15)) w.r.t the detailed fixed point equations in [3], we analyzed each of the 5 test networks using both the original equations, and the simplified equations for several different arrival rates within the uniqueness regime for that

[9]This includes 70 bytes of data, 8 bytes of UDP header, 20 bytes IP header, 27 bytes MAC header, and 6 bytes Phy header.
[10]This restriction was imposed since, in practice, the network planner would like to budget the use of additional relays.

topology.[11] For each topology, we computed the worst case[12] percentage error in the simplified fixed point $\{\overline{\tau}_{-i}\}_{i=1}^{N}$ w.r.t their values obtained from the detailed analysis. We also computed the worst case error in $\max_{1\leq i\leq N}\delta_i$, the maximum packet discard probability over all the nodes in the network. Note that when $\max_{1\leq i\leq N}\delta_i \leq 0.002$, even an absolute error of 0.0005 would result in a percentage error of 25%. We, therefore, adopt the following convention for reporting the errors in $\max_{1\leq i\leq N}\delta_i$. For arrival rates at which $\max_{1\leq i\leq N}\delta_i \leq 0.002$, we report the worst case *absolute* error; for arrival rates at which $\max_{1\leq i\leq N}\delta_i > 0.002$, we report the worst case *percentage* error. Finally, we also computed the worst case percentage error in the end-to-end probability of delivery. Table 1 summarizes the results.

Table 1: Worst case (over all nodes and all arrival rates) errors of the simplified vector fixed point scheme w.r.t the original fixed point scheme in the uniqueness regime

Topology	Node count	Total hop count	% error in $\overline{\tau}_{-i}$	Absolute error in $\max_{1\leq i\leq N}\delta_i$ for $\max_{1\leq i\leq N}\delta_i \leq 0.002$	% error in $\max_{1\leq i\leq N}\delta_i$ for $\max_{1\leq i\leq N}\delta_i > 0.002$	% error in end-to-end delivery probability	% error in end-to-end delay
1	14	36	8.09	.00026	10.5	.1095	5.1
2	10	25	10.05	.00007	0.7	.0236	4.98
3	12	26	9.85	.00016	4.74	.0492	5.7
4	12	27	8.29	.00022	5.76	.0739	4.83
5	12	22	9.77	.00015	5.33	.0487	5.6

Observations:

1. The error in $\overline{\tau}_{-i}$ never exceeded 10.05%.
2. The error in $\max_{1\leq i\leq N}\delta_i$ never exceeded 6% in the regime where $\max_{1\leq i\leq N}\delta_i > 0.002$.
3. The error in end-to-end delay never exceeded 6%.
4. The error in end-to-end delivery probability was negligibly small over the entire uniqueness regime, never exceeding 0.11%, i.e., *the simplified fixed point equations predicted the end-to-end delivery probability extremely accurately*.

Remark: In this paper, we have chosen to compare the results obtained from our simplified fixed point equations against those obtained from the detailed fixed point equations in [3] as opposed to comparing against simulations of the original system, which would be more time consuming. The detailed fixed point equations were shown to be very accurate (well within 10% compared to simulations) in the regime where the discard probability on a link is close to the link PER. Thus, in this low discard regime, an error of 10% w.r.t the detailed equations translates to an error of at most 19%-21% w.r.t the original system.

7.2.2. Validity of the equality assumption

The numerical experiments leading to Observation 1 were conducted as follows: we analyzed each of the 5 test networks using the detailed analysis in [3](also described in Section II-B2 of [2]) to obtain the vector $\{\overline{\tau}_{-i}\}_{i=1}^{N}$ for several different arrival rates ranging from 0.001 pkts/sec to 4 pkts/sec. Then, we computed Jain's fairness index ([26]) for each of these vectors. The Jain's fairness index, $J(\mathbf{x})$, is a measure of fairness (equality) among the components in a

[11] Since we are considering equal arrival rates at all the sources, the uniqueness regime for a particular network is given by an upper bound on the arrival rate λ determined by the R.H.S of Eqn. (15), and the total hop count of the concerned network.

[12] By "worst case", we mean, over all nodes and all arrival rates

given vector $\mathbf{x} = \{x_1, \ldots, x_N\}$. In particular, *closer the value of $J(\mathbf{x})$ to 1, better is the fairness among the components*. As it turned out, in all our experiments, $J(\{\overline{\tau}_{-i}\}_{i=1}^{N}\}) \gg \frac{N-1}{N}$, and within 1.5% of 1, indicating that the components were indeed roughly equal. The results are summarized in Table 2, where, for compact representation, we have reported, for each topology, the *least* value of the fairness index over all the arrival rates.

Table 2: Validation of Observation 1, using Jain's Fairness Index; fairness index of 1 implies exact equality

Topology	Node count	Worst case fairness index
1	14	0.99608
2	10	0.98741
3	12	0.99334
4	12	0.99536
5	12	0.99314

7.2.3. Discussion on the validity of assumptions (A1)-(A5)

Note that assumptions (A1)-(A5) are idealizations made primarily for mathematical convenience. These assumptions are never satisfied exactly in practice, and this is reflected in the fact that the simplified fixed point equations obtained using these assumptions incur additional error with respect to the original detailed fixed point equations. However, as our numerical experiments in Section 7.2.1 suggest, the error incurred by the simplified fixed point equations with respect to the detailed fixed point equations is no more than 10% in the uniqueness regime; this indicates that the assumptions (A1)-(A5) cannot be wildly inaccurate in this regime. In this section, we further investigate, to what extent the idealizations in assumptions (A1)-(A5) are violated in the solution to the detailed fixed point equations in the uniqueness regime.

To do this, we proceeded in the same manner as in Section 7.2.1, and analyzed each of the five test networks using the detailed fixed point analysis for several different arrival rates within the uniqueness regime. For each topology, we computed the worst case (over all nodes, and all arrival rates) values of the following quantities: $1 - \delta_i$, $1 - \gamma_i$, $1 - q_i$, and $1 - c_i$. Note that if assumptions (A1)-(A5) were exactly true, the values of each of these quantities would be exactly 1. Also observe that the error in $1 - r_i$ is always less than that in $1 - \gamma_i$. Hence, we do not report the values of $1 - r_i$ separately. Table 3 summarizes our findings.

Table 3: Worst case (over all nodes and all arrival rates) values of the quantities in assumptions (A1)-(A5) in the original fixed point scheme in the uniqueness regime; ideally, these values would be 1

Topology	$1 - \delta_i$	$1 - \gamma_i$	$1 - q_i$	$1 - c_i$
1	0.9983	0.9431	0.91	0.9
2	0.9998	0.9576	0.9021	0.9053
3	0.9996	0.9549	0.9081	0.9014
4	0.9988	0.9466	0.9012	0.9
5	0.9998	0.9574	0.9013	0.9007

Observations:

1. Assumption (A1) (i.e., $\delta_i \approx 0$) is accurate within 0.17%.
2. Assumption (A5) (i.e., $1 - \gamma_i \approx 1$), and hence (A2) (i.e., $r_i \ll 1$) are accurate within 5.6%.
3. Assumption (A3) (i.e., $q_i \ll 1$) is accurate within 9.8%.
4. Assumption (A4) (i.e., $c_i \approx 0$) is accurate within 10%.
5. Finally, recall from Section 7.2.1 that the overall loss of accuracy in the simplified fixed point equations w.r.t the detailed fixed point equations due to violation of these idealizations is within 10%.

7.3. Throughput optimality of the shortest path tree

To verify the throughput performance of shortest path trees, we generated 60 random instances, each with 10 sources, and 30 potential relay locations deployed uniformly over a $150 \times 150\, m^2$ area. For brevity, we report detailed results from 5 instances here; the observations from the other instances were similar.

7.3.1. Comparison against competing topologies

We are looking for a design that uses a small number of nodes and has a large throughput region for the given target QoS. Since an exhaustive search for the optimal throughput over all possible Steiner trees is computationally impractical, we proceeded as follows to compute an estimate of the optimal throughput for each instance.

Intuitively, two topological properties can affect the throughput of a given network, namely, the total hop count (i.e., the total load in the network), and the number of nodes in the network. Since the SPT gives the least total hop count, clearly there is no need to look at designs that use more relays than an SPT. Hence, for each instance, we first constructed an arbitrary shortest path tree, T_{SPT}, connecting the sources to the sink. Let n_{SPT} be the number of relays in this SPT. We then generated many other candidate Steiner trees as follows: for each $n \in \mathbb{N}$ such that $0 \leq n \leq n_{\text{SPT}}$, we considered all possible combinations of n relays, and with each of these combinations, we constructed a shortest path tree connecting the sources to the sink. If the resulting tree violated the hop constraint $h_{\max} = 5$, it was discarded; otherwise, it was accepted as a candidate solution.

For the chosen QoS targets (see Section 7.1), we analyzed each of these candidate trees using the detailed analysis (Section II-B2 in [2]) for increasing arrival rates, starting from 0.001 pkts/sec, and obtained the maximum arrival rate up to which the target discard probability and mean delay requirements were met. The maximum value of this arrival rate among all the candidate trees was taken as the estimate for the optimal throughput for that instance. Let us denote this as $\hat{\lambda}^{\star}$. This was compared against the throughput achieved by the initially constructed SPT, T_{SPT}, obtained using the detailed analysis in the same manner as described above, and denoted by $\hat{\lambda}^{\text{SPT}}$. *For all the 5 instances, it turned out that* $\hat{\lambda}^{\text{SPT}} = \hat{\lambda}^{\star}$. The results are summarized in Table 4.

Table 4: Verification of throughput optimality of shortest path tree

Scenario	Maximum throughput among candidate trees (including T_{SPT}) $\hat{\lambda}^{\star}$(pkts/sec)	Maximum throughput of T_{SPT} $\hat{\lambda}^{\text{SPT}}$(pkts/sec)
1	5	5
2	4	4
3	3	3
4	5	5
5	5	5

As an illustration, we depict in Figure 5, the network layout of Scenario 2 (left panel of Figure 5), the shortest path tree constructed from this network graph to connect the sources to the sink (middle panel of Figure 5), and also one of the other candidate tree topologies that connects the sources to the sink using just one relay (right panel of Figure 5). It turns out from the numerical experiments that the shortest path tree achieves a throughput of 4 packets/sec from each source (as already mentioned in Table 4), while the other candidate topology depicted in Figure 5 achieves a throughput of 3 packets/sec from each source. The corresponding values from our approximate inner bound formula can be calculated to be 2.8 packets/sec and 2.375 packets/sec respectively.

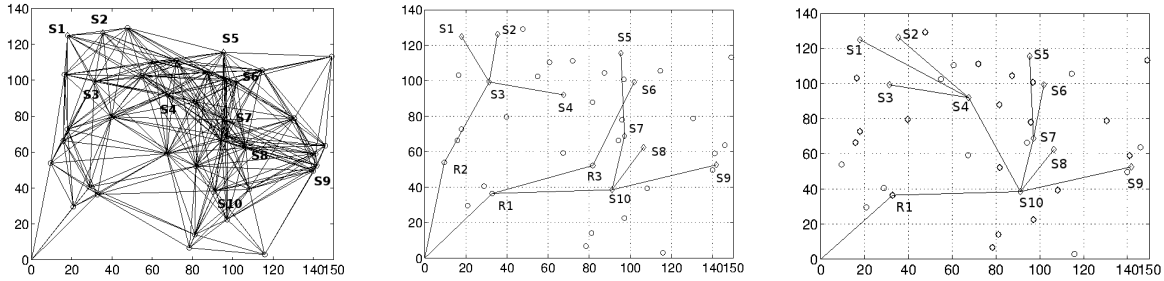

Figure 5: Depiction of the network graph, and two candidate topologies for Scenario 2. Left panel: The network layout, consisting of 10 sources, and 30 potential relay locations. The BS is at (0,0). Each edge has a PER of at most 2%. Middle panel: A shortest path tree connecting the sources to the BS. Note that it uses three relays (R1, R2, and R3). Right panel: a competing tree topology connecting the sources to the sink using just one relay (namely, R1). Note that it has a higher total hop count compared to the shortest path tree.

7.3.2. Comparison against the outcome of the SPTiRP algorithm [1]

For each instance, we also computed a hop count feasible Steiner tree, T_{SPTiRP} using the SPTiRP algorithm proposed in [1] (T_{SPT} was used as the initial feasible solution in running the SPTiRP algorithm). *The idea is to check how much we gain in terms of throughput by using a shortest path design (without any constraint on the number of relays used) instead of the SPTiRP design which uses a nearly minimum number of relays*. Hence, for this Steiner tree also, we computed its throughput using the detailed analysis in the same manner as described above. Furthermore, for the chosen QoS targets, we computed the inner bound on the throughput (maximum arrival rate) as predicted by our approximate formula for both T_{SPT} and T_{SPTiRP}. The results are summarized in Table 5.

Table 5: Throughput comparison of the shortest path tree and the SPTiRP design

Scenario	Predicted $\lambda_{\max}$(pkts/sec) from formula		$\lambda_{\max}$(pkts/sec) from detailed analysis	
	T_{SPTiRP}	T_{SPT}	T_{SPTiRP}	T_{SPT}
1	2.605	3.511	3.5	5
2	2.375	2.785	3	4
3	2.019	2.243	2.9	3
4	3.106	3.67	4	5
5	2.884	3.67	4	5

From Table 5, we observe the following:

1. As we had predicted, the shortest path tree always achieved better throughput than the outcome of the SPTiRP algorithm.
2. However, even the SPTiRP design *can operate at a significant positive load*, while possibly saving on the number of relays used. Hence, when relays are costly, the design based on the SPTiRP algorithm can be used instead of the shortest path tree without much loss in throughput.
3. Finally, comparing column 2 against column 4, and column 3 against column 5, we observe that the inner bound on the throughput region ($\tilde{\Lambda}_{\bar{\delta},\bar{d}}$) predicted by our formula are within 30% of the throughput region obtained using the detailed analysis ($\hat{\Lambda}_{\bar{\delta},\bar{d}}$).

Remarks:

1. We have also performed numerical experiments to see what happens to the QoS performance of the shortest path tree when the arrival rates at the sources are independently subjected to small deviations from the maximum

equal throughput. It was observed that small deviations in the arrival rates from the maximum sustainable equal arrival rate have no significant impact on the QoS performance of the shortest path tree. See [2] for details.

2. Furthermore, we have performed experiments with actual motes to see whether our analytical predictions hold good in an actual network built from off-the-shelf hardware and software. It was observed that for each of the tested topologies, the measured packet delivery probability at the arrival rate predicted by our analysis actually exceeds the packet delivery probability predicted from the target per link discard probability and the maximum number of hops, thus further validating the analytical model. See [2] for details.

7.4. Sensitivity of the bounds to protocol parameters

Finally, it is interesting to ask how the bounds derived in Sections 4 and 5 vary with the parameters of the protocol, namely, (i) n_c, the maximum number of CCA failures before packet discard, (ii) n_t, the maximum number of transmission failures before packet discard, and (iii) the minimum back-off exponent [4], which determines the range from which the first random back-off, and hence the subsequent random back-offs are sampled; *this affects only the mean delay, and hence the bound $B'(\overline{\delta}, \overline{d})$, but does not affect $B(\overline{\delta})$.*

To test the effect of each of these protocol parameters, we fixed the other protocol parameters at their default values (as specified in [4]), and varied the concerned parameter over a reasonable range, and for each value of the parameter, we computed $B(\overline{\delta})$, and $B'(\overline{\delta}, \overline{d})$. For lack of space, we only summarize the main observations here; see [2] for detailed results and explanations.

Observations:

1. $B(\overline{\delta})$ increases in n_c up to $n_c = 4$, then decreases in n_c, whereas $B'(\overline{\delta}, \overline{d})$ is monotonically decreasing in n_c.
2. For the entire tested range of n_t, $B(\overline{\delta})$ is invariant of n_t. $B'(\overline{\delta}, \overline{d})$ is monotonically decreasing in n_t.
3. $B'(\overline{\delta}, \overline{d})$ is monotonically decreasing in the minimum backoff exponent.

8. Conclusion

In this paper, we have studied the problem of QoS aware network design under a class of CSMA/CA protocols including IEEE 802.15.4 CSMA/CA. Assuming that there are no hidden terminals in the network, we have derived a simplified set of fixed point equations from the more elaborate analysis developed in [3]. We have proved the uniqueness of the fixed point of our proposed equations, and verified through numerical experiments, their accuracy w.r.t the detailed analysis in [3]. From these simplified equations, we have derived an approximate inner bound on the QoS respecting throughput region of a given tree network where the QoS requirements are, a target discard probability on each link, and a target mean delay on each link (obtained by equally splitting the end-to-end QoS objectives over the links in a source-sink path). The structure of our inner bound sheds light on the dependence of the network performance on topological properties, and the arrival rate vector. In particular, our results indicate that to achieve a target per hop discard probability (respectively, mean delay), it suffices to control the total load, $\sum_{k=1}^{m} \lambda_k h_k$, (respectively, the maximum load over all nodes, $\max_{1 \le i \le N} \nu_i$) in the network. Furthermore, for the special case of default backoff parameters of IEEE 802.15.4, equal arrival rates at all sources, and reasonable values of QoS targets,

we have argued that controlling the total load is enough to meet both the discard probability and the mean delay targets. Under the same special case, we have also shown that the shortest path tree achieves the maximum throughput among all topologies that satisfy the approximate sufficient condition to meet the QoS targets.

In our ongoing work, we aim to extend these results to the more general case where there are hidden terminals in the network.

9. Appendix

9.1. An algorithm for Steiner tree construction with hop constraint $h_{\max}$ and relay count constraint $N_{\max}$

1. Run the SPTiRP algorithm (proposed in [1]) on the graph G until the relay count in the resulting solution is $\leq N_{\max}$, or the hop constraint is violated for some source. If the resulting solution is feasible, retain it as a candidate solution, and compute its total hop count.
2. Repeat Step 1 for a fixed number of iterations, each time starting with a randomly chosen SPT as the initial solution.
3. Pick the candidate solution with the least total hop count.

9.2. Proof of Proposition 1

We begin by establishing the following result, which will be used to prove the main result.

Lemma 4. *Let $f = (f_1, f_2, \ldots, f_N) : [0,a]^N \to [0,a]^N$ be such that for all $\mathbf{x} \in [0,a]^N$, and for all $i = 1, \ldots, N$, $f_i(\mathbf{x}) = \sum_{j \neq i} g_j(x_j)$, where $g_j : [0,a] \to \mathbb{R}_+$ is Lipschitz continuous with Lipschitz constant L_j for each j, $1 \leq j \leq N$, and $\sum_{j=1}^{N} L_j < 1$. Then, the fixed point equations $\mathbf{x} = f(\mathbf{x})$ have a unique solution in $[0,a]^N$.*

Proof. By our hypothesis, f maps $[0,a]^N$ into $[0,a]^N$. We shall show that under the hypotheses, f is a contraction on $[0,a]^N$ w.r.t the metric d which is defined as $d(\mathbf{x},\mathbf{y}) = \max\limits_{1 \leq i \leq N} |x_i - y_i| \; \forall \mathbf{x}, \mathbf{y} \in [0,a]^N$. Then, since $[0,a]^N$ is complete w.r.t the metric d, the uniqueness of the fixed point follows from Banach's fixed point theorem [27].

Let $\mathbf{x}_1, \mathbf{x}_2 \in [0,a]^N$. Then, for all $i = 1, \ldots, N$,

$$
\begin{aligned}
|f_i(\mathbf{x}_1) - f_i(\mathbf{x}_2)| &= \left| \sum_{j \neq i} (g_j(x_{1,j}) - g_j(x_{2,j})) \right| \\
&\leq \sum_{j \neq i} |g_j(x_{1,j}) - g_j(x_{2,j})| \\
&\leq \sum_{j \neq i} L_j |x_{1,j} - x_{2,j}| \qquad (21) \\
&\leq \left(\sum_{j \neq i} L_j \right) \max_{1 \leq j \leq N} |x_{1,j} - x_{2,j}| \\
&= \left(\sum_{j \neq i} L_j \right) d(\mathbf{x}_1, \mathbf{x}_2) \\
&\leq \left(\sum_{j=1}^{N} L_j \right) d(\mathbf{x}_1, \mathbf{x}_2)
\end{aligned}
$$

where, in (21), we have used the Lipschitz continuity of $g_j(\cdot)$.

It follows that

$$\begin{aligned} d(f(\mathbf{x}_1), f(\mathbf{x}_2)) &= \max_{1\le i\le N} |f_i(\mathbf{x}_1) - f_i(\mathbf{x}_2)| \\ &\le (\sum_{j=1}^{N} L_j) d(\mathbf{x}_1, \mathbf{x}_2) \\ &=: K d(\mathbf{x}_1, \mathbf{x}_2) \end{aligned}$$

where, $K = \sum_{j=1}^{N} L_j < 1$ by the hypothesis of the lemma. Thus, f is a contraction on $[0, a]^N$. This completes the proof of the lemma. □

Proof of Proposition 1:

Using the notation of Lemma 4, let, for all $i = 1, \ldots, N$, $j = 1, \ldots, N$, $x_i = \overline{\tau}_{-i}$, $g_j(x_j) = \nu_j(1 + \alpha_j + \ldots + \alpha_j^{n_c-1})$, with $\alpha_j = \frac{T_{tx} x_j}{1+T_{tx} x_j}$, and $f_i(\mathbf{x}) = \sum_{j\neq i} g_j(x_j)$. Then, our simplified fixed point equations (3), (4) are of the form $\mathbf{x} = f(\mathbf{x})$, where $f = (f_1, \ldots, f_N)$.

Let $\mathbf{x} \in [0, a]^N$ with $a = \frac{\alpha_{\max}}{T_{\text{tx}}(1-\alpha_{\max})}$ and $\alpha_{\max} = \overline{\delta}^{1/n_c}$. Then, $\alpha_j \le \alpha_{\max}$ for all $j = 1, \ldots, N$, and we have

$$\begin{aligned} f_i(\mathbf{x}) &= \sum_{j\neq i} \nu_j(1 + \alpha_j + \ldots + \alpha_j^{n_c-1}) \\ &\le (1 + \alpha_{\max} + \ldots \alpha_{\max}^{n_c-1}) \sum_{j\neq i} \nu_j \\ &\le (1 + \alpha_{\max} + \ldots \alpha_{\max}^{n_c-1}) \sum_{j=1}^{N} \nu_j \\ &= (1 + \alpha_{\max} + \ldots \alpha_{\max}^{n_c-1}) \sum_{k=1}^{m} \lambda_k h_k, \text{ using (A1)} \\ &\le a \end{aligned}$$

where, in the last step, we have used the hypothesis that $\sum_{k=1}^{m} \lambda_k h_k < \frac{a}{1+\alpha_{\max}+\ldots\alpha_{\max}^{n_c-1}}$. Thus, $f(\cdot)$ maps $[0, a]^N$ *into* $[0, a]^N$.

Next we investigate the functions $g_j(\cdot)$, $j = 1, \ldots, N$. Let $\mathbf{x}_1, \mathbf{x}_2 \in [0, a]^N$. Let $\alpha_{1,j}$ and $\alpha_{2,j}$ be the values of α_j

corresponding to $\mathbf{x}_1$ and $\mathbf{x}_2$ respectively. Then, $\alpha_{1,j}, \alpha_{2,j} \leq \alpha_{\max}$ for all $j = 1, \ldots, N$, and we have

$$\begin{aligned}
|g_j(x_{1,j}) - g_j(x_{2,j})| &= \nu_j |\alpha_{1,j} - \alpha_{2,j}| \times (1 + \sum_{k=1}^{n_c-2} \sum_{l=0}^{k} \alpha_{1,j}^{k-l} \alpha_{2,j}^{l}) \\
&\leq \nu_j (1 + 2\alpha_{\max} + \ldots + (n_c - 1)\alpha_{\max}^{n_c-2}) \\
&\times |\alpha_{1,j} - \alpha_{2,j}| \\
&\leq \nu_j T_{tx} (1 + 2\alpha_{\max} + \ldots + (n_c - 1)\alpha_{\max}^{n_c-2}) \\
&\times |x_{1,j} - x_{2,j}| \\
&= L_j |x_{1,j} - x_{2,j}|
\end{aligned}$$

where, $L_j =: \nu_j T_{tx}(1 + 2\alpha_{\max} + \ldots + (n_c - 1)\alpha_{\max}^{n_c-2})$. Thus, $g_j(\cdot)$ is Lipschitz continuous with Lipschitz constant L_j for all $j = 1, \ldots, N$. Moreover, we have

$$\begin{aligned}
\sum_{j=1}^{N} L_j &= T_{tx}(1 + 2\alpha_{\max} + \ldots + (n_c - 1)\alpha_{\max}^{n_c-2}) \sum_{j=1}^{N} \nu_j \\
&= T_{tx}(1 + 2\alpha_{\max} + \ldots + (n_c - 1)\alpha_{\max}^{n_c-2}) \sum_{k=1}^{m} \lambda_k h_k \\
&< 1
\end{aligned}$$

where the last step follows from the condition that $\sum_{k=1}^{m} \lambda_k h_k < \frac{1}{T_{tx}(1+2\alpha_{\max}+\ldots+(n_c-1)\alpha_{\max}^{n_c-2})}$.

Thus, we see that all the conditions of Lemma 4 are satisfied by the simplified fixed point equations in $[0, a]^N$. Hence, by Lemma 4, the simplified fixed point equations have a unique solution in $[0, a]^N$. □

9.3. Proof of Proposition 3

To prove the existence and uniqueness of the scalar fixed point equation, we shall need one more analytical result, which we state below.

Lemma 5. *Let $a \in \mathbb{R}_+$. Suppose $f : [0, a] \to [0, a]$ such that f can be expressed as $f(\cdot) = Mg(\cdot)$, where $M > 0$, and $g : [0, a] \to \mathbb{R}_+$ is a Lipschitz continuous function with Lipschitz constant L such that $ML < 1$. Then,*

1. *The fixed point equation $x = f(x)$ has a unique solution in $[0, a]$.*
2. *Let us denote this unique fixed point as $h(M)$, to indicate its dependence on M. Suppose now that $g(\cdot)$ is differentiable on $(0, a)$. Then, $h(M)$ is continuous, and monotonically increasing in M.*
3. *Suppose further that $g \in C^1$, i.e., $g'(\cdot)$ is continuous. Then, $h(\cdot)$ is differentiable.*

Proof. 1. By hypothesis, f maps $[0, a]$ into $[0, a]$. We shall show that under the condition $ML < 1$, $f(\cdot)$ is a contraction on $[0, a]$ w.r.t $|\cdot|$. Then, since $[0, a]$ is a complete metric space, it follows from Banach's fixed point theorem that the fixed point equation has a unique solution in $[0, a]$.

Consider $x_1, x_2 \in [0, a]$. Then,

$$\begin{aligned}\left|f(x_1) - f(x_2)\right| &= M|g(x_1) - g(x_2)| \\ &\leq ML|x_1 - x_2| \\ &= C|x_1 - x_2|\end{aligned}$$

where, $C =: ML < 1$. Thus, f is a contraction. Hence the proof.

2. We have, $h(M) = Mg(h(M))$. Then, for $M > 0$, and non-zero ϵ (small enough such that $M + \epsilon > 0$),

$$\begin{aligned}h(M+\epsilon) - h(M) &= (M+\epsilon)g(h(M+\epsilon)) - Mg(h(M)) \\ &= M[g(h(M+\epsilon)) - g(h(M))] \\ &+ \epsilon g(h(M+\epsilon)) \\ &= M[\{h(M+\epsilon) - h(M)\}g'(\xi)] \\ &+ \epsilon g(h(M+\epsilon)) \qquad (22) \\ &= Mg'(\xi)[h(M+\epsilon) - h(M)] \\ &+ \epsilon g(h(M+\epsilon))\end{aligned}$$

where, (22) follows from the Mean Value Theorem, with ξ lying between $h(M)$ and $h(M + \epsilon)$. Thus, we have,

$$\begin{aligned}h(M+\epsilon) - h(M) &= \frac{\epsilon g(h(M+\epsilon))}{1 - Mg'(\xi)} \\ &= \frac{\epsilon \frac{h(M+\epsilon)}{M+\epsilon}}{1 - Mg'(\xi)} \qquad (23)\end{aligned}$$

Note that for $\epsilon > 0$, the R.H.S of Equation (23) is *non-negative*, since $Mg'(\xi) \leq M|g'(\xi)| \leq ML < 1$, and $h(\cdot) \geq 0$. Thus, it follows that $h(M)$ is monotonically increasing in M.

To show that $h(\cdot)$ is continuous in M, we proceed as follows. Since the denominator of the R.H.S of (23) is non-negative for $ML < 1$, we have, from (23),

$$\begin{aligned}|h(M+\epsilon) - h(M)| &= \frac{|\epsilon|\left|\frac{h(M+\epsilon)}{M+\epsilon}\right|}{1 - Mg'(\xi)} \\ &\leq \frac{\left|\frac{\epsilon}{M+\epsilon}\right||h(M+\epsilon)|}{1 - ML} \\ &\leq \frac{\left|\frac{\epsilon}{M+\epsilon}\right|}{1 - ML}a, \text{ since } h(M+\epsilon) \in [0, a]\end{aligned}$$

Thus, for any given $\delta > 0$, $|h(M+\epsilon) - h(M)| < \delta$ whenever $\left|\frac{\epsilon}{M+\epsilon}\right| < \frac{1-ML}{a}\delta =: t(\delta)$. Without loss of generality[13], we take $\delta < \frac{a}{1-ML}$ so that $t(\delta) < 1$. Then, $\left|\frac{\epsilon}{M+\epsilon}\right| < t(\delta) \Leftrightarrow -t(\delta) < \frac{\epsilon}{M+\epsilon} < t(\delta)$, which yields, after some algebraic manipulations, $\frac{-Mt(\delta)}{1+t(\delta)} < \epsilon < \frac{Mt(\delta)}{1-t(\delta)}$. This holds whenever $|\epsilon| < \frac{Mt(\delta)}{1+t(\delta)}$. Hence, the continuity of $h(\cdot)$ follows.

3. From Eqn.23, we have

$$\frac{h(M+\epsilon) - h(M)}{\epsilon} = \frac{\frac{h(M+\epsilon)}{M+\epsilon}}{1 - Mg'(\xi)}$$

Taking limits on both sides as $\epsilon \to 0$, and using the continuity of $h(\cdot)$ and $g'(\cdot)$, we have

$$h'(M) = \frac{h(M)/M}{1 - Mg'(h(M))} \tag{24}$$

since ξ lies between $h(M+\epsilon)$ and $h(M)$. This completes the proof.

□

Proof of Proposition 3: Using the notation of Lemma 5, let us write $x = \overline{\tau}$, $M = \sum_{k=1}^{m} \lambda_k h_k$, $g(x) = 1 + \alpha + \ldots + \alpha^{n_c-1}$, and $f(x) = Mg(x)$, where $\alpha = \frac{T_{tx}x}{1+T_{tx}x}$. Then, using a derivation similar to the one in the proof of Proposition 1, it can be seen that $f(\cdot)$ maps $[0, a]$ into $[0, a]$ under the condition $\sum_{k=1}^{m} \lambda_k h_k < \frac{a}{1+\alpha_{\max}+\ldots+\alpha_{\max}^{n_c-1}}$.

Let $x_1, x_2 \in [0, a]$. Then,

$$\begin{aligned}
|g(x_1) - g(x_2)| &= |\alpha_1 - \alpha_2|(1 + \sum_{k=1}^{n_c-2}\sum_{l=0}^{k} \alpha_1^{k-l}\alpha_2^{l}) \\
&\leq (1 + 2\alpha_{\max} + \ldots + (n_c-1)\alpha_{\max}^{n_c-2})|\alpha_1 - \alpha_2| \\
&\leq T_{tx}(1 + 2\alpha_{\max} + \ldots + (n_c-1)\alpha_{\max}^{n_c-2})|x_1 - x_2| \\
&= L|x_1 - x_2|
\end{aligned}$$

where, $L =: T_{tx}(1+2\alpha_{\max}+\ldots+(n_c-1)\alpha_{\max}^{n_c-2})$. Thus, $g(\cdot)$ is Lipschitz continuous with Lipschitz constant L. Moreover, under the condition given by (15), $ML = (\sum_{k=1}^{m} \lambda_k h_k)T_{tx}(1 + 2\alpha_{\max} + \ldots + (n_c-1)\alpha_{\max}^{n_c-2}) < 1$. Hence, from Part 1 of lemma 5, it follows that the scalar fixed point equation defined by (16), (17) has a unique solution in $[0, a]$.

9.4. Proof of Proposition 4

Proof. Recall from the proof of Proposition 1 that the function describing the vector fixed point equations is a contraction on $[0, a]^N$, where a is as defined in Sections 3.4 and 4.3. Hence, an iterative procedure starting with any initial solution in $[0, a]^N$ will converge to the unique fixed point $\{\overline{\tau}_{-i}\}_{i=1}^{N}$.

[13] any ϵ that works for such a δ also works for higher values of δ

Let us initialize the iteration with $\overline{\tau}_{-i}^{(0)} = \overline{\tau}$ for all $i = 1, \ldots, N$. Note that this initial solution is in $[0, a]^N$. Then, from eqns. (4) and (17), we have $\alpha_i^{(0)} = \alpha$ for all $i = 1, \ldots, N$. Thus, for all $i = 1, \ldots, N$,

$$\begin{aligned}
\overline{\tau}_{-i}^{(1)} &= \sum_{j \neq i} \nu_j (1 + \alpha_j^{(0)} + \ldots + (\alpha_j^{(0)})^{n_c - 1}), \text{ where } \nu_j = \sum_{k=1}^{m} z_{k,j} \lambda_k \\
&= (1 + \alpha + \ldots + \alpha^{n_c - 1}) \sum_{j \neq i} \nu_j \\
&\leq (1 + \alpha + \ldots + \alpha^{n_c - 1}) \sum_{j=1}^{N} \nu_j \\
&= (\sum_{k=1}^{m} \lambda_k h_k)(1 + \alpha + \ldots + \alpha^{n_c - 1}) \\
&= \overline{\tau} \\
&= \overline{\tau}_{-i}^{(0)}
\end{aligned} \tag{25}$$

Now, we use induction to complete the proof. Suppose, for some iteration k, we have, for all $i = 1, \ldots, N$, $\overline{\tau}_{-i}^{(k)} \leq \overline{\tau}_{-i}^{(k-1)}$. Then, since the R.H.S of (4) is monotonically increasing in $\overline{\tau}_{-i}$, it follows that for all $i = 1, \ldots, N$, $\alpha_i^{(k)} \leq \alpha_i^{(k-1)}$. Hence, for all $i = 1, \ldots, N$,

$$\begin{aligned}
\overline{\tau}_{-i}^{(k+1)} &= \sum_{j \neq i} \nu_j (1 + \alpha_j^{(k)} + \ldots + (\alpha_j^{(k)})^{n_c - 1}) \\
&\leq \sum_{j \neq i} \nu_j (1 + \alpha_j^{(k-1)} + \ldots + (\alpha_j^{(k-1)})^{n_c - 1}) \\
&= \overline{\tau}_{-i}^{(k)}
\end{aligned}$$

Thus, when the monotonicity property of the iterates holds for iteration k, it also holds for iteration $(k + 1)$. From (25), it holds for $k = 1$. Hence, by induction, it holds for all iterations. Since the iterates converge to the unique fixed point $\{\overline{\tau}_{-i}\}_{i=1}^{N}$, it follows that for all $i = 1, \ldots, N$, $\overline{\tau}_{-i} \leq \overline{\tau}_{-i}^{(0)} = \overline{\tau}$. This completes the proof. □

9.5. Detailed fixed point equations for NH case (extracted from [3])

Assuming that the CCA attempt process at each node i, conditioned on the node being in backoff, is distributed as $\exp(\beta_i)$, the CCA failure probability, α_i, of node i is given by

$$\alpha_i = \frac{(1 - \eta_i)(1 - c_i)\beta_i T_{tx}}{\eta_i + (1 - \eta_i)c_i + (1 - \eta_i)(1 - c_i)\beta_i T_{tx}} \tag{26}$$

where, T_{tx} is the packet transmission duration, η_i is the probability that node i finishes its backoff first, and c_i is the probability that node i finishes its backoff within 12 symbol times (the turnaround time) after another node finishes its backoff. This equation can be interpreted as a consequence of the Renewal-Reward Theorem (RRT)(e.g., see [24]) as follows: the numerator is the mean number of failed CCA attempts by node i in a renewal cycle (see Figure 3), and the denominator is the mean number of total CCA attempts by node i in a renewal cycle.

$$\eta_i = \frac{\beta_i}{\beta_i + \sum_{j \neq i} \overline{\tau}_j^{(i)}}$$

$$c_i = \left(1 - e^{-12\beta_i}\right)$$

where, $\overline{\tau}_j^{(i)}$ is the CCA attempt rate of node j *conditioned on the times during which it is either empty or in backoff*, and is given by

$$\overline{\tau}_j^{(i)} = \frac{\beta_j \times b_j \times q_j}{1 - q_j + q_j \times b_j} \tag{27}$$

where, b_j is the fraction of time node j is in backoff given that it is non-empty, and q_j is the probability that node j is non-empty. The above expression can be interpreted as a consequence of the RRT: the numerator is the mean number of CCA attempts by node j in a renewal cycle, and the denominator is the mean time during which the node j is not transmitting in a renewal cycle (both obtained after normalizing the renewal cycle length to unity). Also, note that at the start of the renewal cycle, node j can be either empty, or in backoff (i.e., it cannot be transmitting); hence $\overline{\tau}_j^{(i)}$ is also the CCA attempt rate of node j *as perceived by the tagged node* i. We also have,

$$b_i = \frac{\overline{B}_i}{\overline{B}_i + (1 - \alpha_i^{n_c}) T_{\mathsf{tx}}} \tag{28}$$

where, we recall that $\overline{B}_i$ is the mean time spent in backoff by the HOL packet at node i before it is transmitted, or gets discarded due to successive CCA failures. The denominator of the expression for b_i can then be easily intrepreted as the mean time that node i is non-empty in a renewal cycle; this provides an intuitive explanation for the expression for b_i.

The node non-empty probability, q_i, can be written, using Little's theorem as

$$q_i = \min\{1, \frac{\nu_i}{\sigma_i}\} \tag{29}$$

where, ν_i is the total arrival rate into node i, and $\frac{1}{\sigma_i}$ is the mean service time of the HOL packet at node i.

Recall that $r_i = \gamma_i(1-\alpha_i^{n_c})$ denotes the probability that the HOL packet at node i was transmitted, and it encountered a transmission failure (either due to collision or due to link error).

Then, the mean service time of the HOL packet at node i is given by

$$\frac{1}{\sigma_i} = \overline{Z}_i + \overline{Y}_i \tag{30}$$

where,

$$\overline{Z}_i = \overline{B}_i(1 + r_i + r_i^2 + \ldots + r_i^{n_t-1}) \tag{31}$$

$$\overline{Y}_i = (1 - \alpha_i^{n_c})T_{\mathsf{tx}}(1 + r_i + r_i^2 + \ldots + r_i^{n_t-1}) \tag{32}$$

denote respectively, the mean time spent in backoff by the HOL packet, and the mean time spent in transmission by the HOL packet. Here n_t is the number of transmission failures after which the packet is discarded.

Recall that δ_i is the packet discard probability at node i. Then the total arrival rate into node i is given by

$$\nu_i = \lambda_i + \sum_{k \in \mathcal{P}_i} \theta_k \tag{33}$$

where,

$$\theta_k = \nu_k(1 - \delta_k) \tag{34}$$

is the goodput of node k.

As explained earlier, the analysis of packet delay between a source node and the sink node utilizes the approximation techniques in Whitt's Queueing Network Analyzer (QNA, [23]). The arrival processes at the source nodes are modeled as independent Poisson processes. The end-to-end mean packet delay for a source node j, provided that the set of nodes along the path from this node to the BS is L_j, is given by

$$\Delta_j \quad = \quad \sum_{i \in L_j} \overline{\Delta}_i \tag{35}$$

where, $\overline{\Delta}_i$ is the mean sojourn time at a node i, and is given by the following standard GI/GI/1 approximation:

$$\overline{\Delta}_i \quad = \quad \frac{\rho_i \mathbb{E}(S_i)(c_{A_i}^2 + c_{S_i}^2)}{2(1 - \rho_i)} + \mathbb{E}(S_i) \tag{36}$$

Here, ρ_i denotes the traffic load at node i, S_i denotes the service time at node i, $c_{S_i}^2$ is the squared coefficient of variance of service time at node i, and $c_{A_i}^2$ is the squared coefficient of variance for the interarrival times at node i. We also have,

$$\begin{aligned} c_{S_i}^2 &= \frac{\mathbb{E}(S_i^2)}{(\mathbb{E}(S_i))^2} - 1 \\ \mathbb{E}(S_i) &= -\frac{d(M_{S_i}(z))}{dz}\bigg|_{z=0} \\ \mathbb{E}(S_i^2) &= \frac{d^2(M_{S_i}(z))}{dz^2}\bigg|_{z=0} \end{aligned}$$

where, we recall that $M_{S_i}(z)$ is the MGF of the service time of node i, and can be expressed as,

$$M_{S_i}(z) \quad = \quad \frac{\beta_i(1-\alpha_i)(1-\gamma_i)e^{-zT_{\mathsf{tx}}}}{z+\beta_i(1-\alpha_i)(1-\gamma_i e^{-zT_{\mathsf{tx}}})}.$$

with β_i, α_i, γ_i and T_{tx} having the same interpretation as in Section 3.3.

Further, $c^2_{A_i}$ is calculated as

$$c^2_{A_i} \quad = \quad \frac{1}{\Lambda_i}\left(\lambda_i + \sum_{j\in\mathcal{P}_i}\Lambda_j c^2_{D_j}\right)$$

where, Λ_i is the total arrival rate into Node i, λ_i is the exogeneous Poisson arrival rate into Node i ($\lambda_i = 0$ if Node i is a relay node), $\mathcal{P}_i$ is the set of predecessors of node i, and

$$c^2_{D_i} \quad = \quad (1-\delta_i)(1+\rho_i^2(c^2_{S_i}-1)+(1-\rho_i^2)(c^2_{A_i}-1))$$

is the squared coefficient of variation of the departure process at node i.

9.6. Derivation of the simplified fixed point equations from the detailed fixed point equations under assumptions (A1)-(A5)

In Section 3.3, we had provided a direct intuitive explanation for the simplified fixed point equations in the low discard regime. In this section, we show how these equations can be derived from the detailed fixed point equations under assumptions (A1)-(A5).

Let us define

$$\overline{\tau}_{-i} =: \sum_{j\neq i}\overline{\tau}^{(i)}_j$$

where $\overline{\tau}^{(i)}_j$ is given by Equation (27). Note that $\overline{\tau}_{-i}$ still has the same interpretation as before. Using Equation (27), we have, for all $i = 1,\ldots,N$,

$$\begin{aligned}
\overline{\tau}_{-i} &= \sum_{j\neq i}\frac{\beta_j \times b_j \times q_j}{1-q_j+q_j\times b_j} \\
&\approx \sum_{j\neq i}\beta_j \times b_j \times q_j, \text{ using (A3)} \\
&= \sum_{j\neq i}\frac{1+\alpha_j+\ldots+\alpha_j^{n_c-1}}{\overline{B}_j+(1-\alpha_j^{n_c})T_{\mathsf{tx}}}\nu_j(\overline{Z}_j+\overline{Y}_j) \qquad (37)\\
&\approx \sum_{j\neq i}\nu_j(1+\alpha_j+\ldots+\alpha_j^{n_c-1}) \\
&\approx \sum_{j\neq i}\left(\sum_{k=1}^{m}z_{k,j}\lambda_k\right)(1+\alpha_j+\ldots+\alpha_j^{n_c-1}), \text{ using (A1)}
\end{aligned}$$

In writing Equation (37), we have used Equations (8), (28), (29), and (30). In writing the last step, we have used (A2) along with eqns. 31 and 32 to approximate $\overline{Z}_j + \overline{Y}_j \approx \overline{B}_j + (1 - \alpha_j^{n_c})T_{\text{tx}}$.

Also, from Equation (26), using (A4), we have, for all $i = 1, \ldots, N$,

$$\alpha_i \approx \frac{T_{\text{tx}}\overline{\tau}_{-i}}{1 + T_{\text{tx}}\overline{\tau}_{-i}}$$

Thus, we can write the simplified fixed point equations compactly as follows:

$$\overline{\tau}_{-i} = \sum_{j \neq i} \left(\sum_{k=1}^{m} z_{k,j}\lambda_k \right) (1 + \alpha_j + \ldots + \alpha_j^{n_c - 1}) \; \forall i = 1, \ldots, N \tag{38}$$

$$\alpha_i = \frac{T_{\text{tx}}\overline{\tau}_{-i}}{1 + T_{\text{tx}}\overline{\tau}_{-i}} \; \forall i = 1, \ldots, N \tag{39}$$

Simplifications for the delay approximation

Recall that in the low discard regime, $\delta_i \approx 0$, and $\rho_i \ll 1$ so that $\rho_i^2 \approx 0$. Then it is easy to see that $c_{A_i}^2 \approx 1$. Furthermore, $\rho_i \approx \nu_i \mathbb{E}(S_i)$, where we recall that ν_i is the total arrival rate into node i assuming no packet discard. Thus, we have, from (36),

$$\overline{\Delta}_i = \frac{\rho_i \mathbb{E}(S_i)(1 + c_{S_i}^2)}{2(1 - \rho_i)} + \mathbb{E}(S_i) \tag{40}$$

9.7. A discussion on the no hidden nodes assumption

While the NH assumption may seem restrictive, observe that by using a cluster based network topology where within each cluster, the nodes satisfy the NH assumption, and different channels are used across adjacent clusters (we recall that there are 16 channels available for IEEE 802.15.4 CSMA/CA [4]), moderate to large areas can be covered. One way of constructing such a cluster based topology is explained below.

We assume that each cluster will cover a regular hexagonal region in the plane, and within each cluster, there will be a single BS placed at the center of the hexagon. Suppose the carrier sense range of each node is r_{cs}, and, for a fixed packet size and a given path loss model, the maximum allowed link length to ensure the target link PER l is r. Further suppose that r is chosen such that $r_{\text{cs}} = 2mr$, for some integer $m > 0$.

Having thus chosen r, *we let the length of each side of a hexagonal cluster be* mr. Then, it follows from triangle inequality that all nodes within a hexagonal cluster are within CS range of each other.

Now consider two distinct clusters. Let R be the distance between the BSs in these two clusters. Consider a pair of nodes, one picked from each of these clusters. Let s be the distance between these two nodes. See Figure 6. It follows from triangle inequality that

$$R \leq s + 2mr$$

$$\Rightarrow s \geq R - 2mr$$

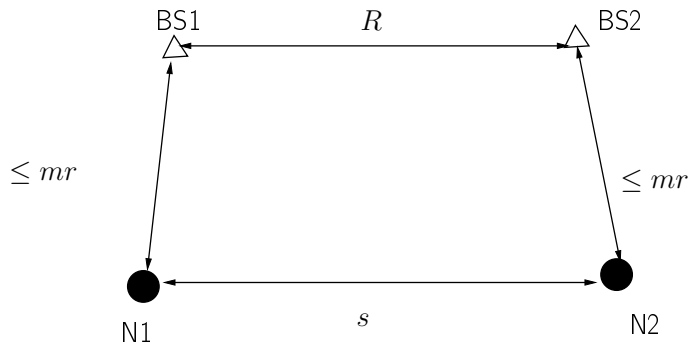

Figure 6: Computation of the minimum distance between nodes in two different clusters

Thus, the distance between any pair of points across the two clusters is at least $R - 2mr$.

We can use the same channel in these two clusters if the nodes in one cluster are completely hidden from those in the other, so that they do not interfere with one another. This is ensured if $R - 2mr \geq r_{cs} = 2mr$. Thus, it suffices to have $R \geq 4mr$. In other words, we can use the same channel in two different clusters if the distance between the BSs in these two clusters is at least $4mr$.

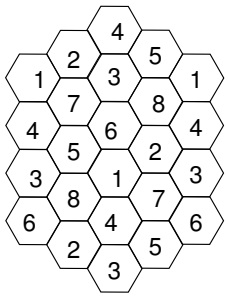

Figure 7: Channel assignment to hexagonal clusters to ensure no interference across clusters

Now consider the channel assignment in the hexagonal cluster layout shown in Figure 7, where the length of each side of each hexagon is mr. It can be verified using elementary geometry that the BSs of any two co-channel clusters are separated by more than $4mr$, and hence with this channel assignment, there is no interference across clusters, while within each cluster, the NH assumption is satisfied. Note than we needed to use only 8 channels out of the available 16 channels.

See also [6] for a more cost-effective strategy to select base stations and relays for such cluster based coverage.

References

[1] A. Bhattacharya, A. Kumar, A shortest path tree based algorithm for relay placement in a wireless sensor network and its performance analysis, Computer Networks 71 (2014) 48–62.

[2] A. Bhattacharya, A. Kumar, An approximate inner bound to the QoS aware throughput region of a tree network under IEEE 802.15.4 CSMA/CA and application to wireless sensor network design, Tech. rep., available at arxiv.org/pdf/1408.1222 (2014).

[3] R. Srivastava, S. M. Ladwa, A. Bhattacharya, A. Kumar, A fast and accurate performance analysis of beaconless IEEE 802.15.4 multi-hop networks, Tech. rep., available at arxiv.org/pdf/1408.1225 (2014).

[4] IEEE, IEEE Standards Part 15.4: Wireless Medium Access Control (MAC) and Physical Layer (PHY) Specifications for Low-Rate Wireless Personal Area Networks (LR-WPANs), New York (October 2003).

[5] S. Misra, S. D. Hong, G. Xue, J. Tang, Constrained Relay Node Placement in Wireless Sensor Networks to Meet Connectivity and Survivability Requirements, in: IEEE INFOCOM, 2008.

[6] A. Bhattacharya, A. Rao, K. P. Naveen, P. P. Nishanth, S. Anand, A. Kumar, QoS constrained optimal sink and relay placement in planned wireless sensor networks, in: 10th IEEE International Conference on Signal Processing and Communications (SPCOM), Bangalore, India, 2014.

[7] R. Srivastava, A. Kumar, Performance Analysis of Beacon-Less IEEE 802.15.4 Multi-Hop Networks, in: 4th International Conference on Communication Systems and Networks (COMSNETS), 2012.

[8] P. Park, C. Fischione, K. H. Johansson, Modeling and Stability Analysis of Hybrid Multiple Access in the IEEE 802.15.4 Protocol, ACM Transactions on Sensor Networks 9 (2).

[9] G. Bianchi, Performance analysis of the IEEE 802.11 distributed coordination function, IEEE Journal on Selected Areas in Communications 18 (2000) 535–547.

[10] A. Kumar, E. Altman, D. Miorandi, M. Goyal, New insights from a fixed point analysis of single cell IEEE 802.11 wireless LANs, IEEE/ACM Transactions on Networking 15 (2007) 588–601.

[11] A. Jindal, K. Psounis, The achievable rate region of 802.11-scheduled multihop networks, IEEE/ACM Transactions on Networking 17 (4).

[12] B. Nardelli, E. W. Knightly, Closed-form throughput expressions for CSMA networks with collisions and hidden terminals, in: IEEE Infocom, 2012.

[13] P. Marbach, A. Eryilmaz, A. Ozdaglar, Asynchronous CSMA policies in multihop wireless networks with primary interference constraints, IEEE Transactions on Information Theory 57 (6).

[14] C. Bordenave, D. McDonald, A. Proutiere, Asymptotic stability region of slotted aloha, IEEE Transactions on Information Theory 58 (9) (2012) 5841–5855.

[15] S. Srinivasa, M. Haenggi, Combining stochastic geometry and statistical mechanics for the analysis and design of mesh networks, Ad Hoc Networks 13 (2014) 110–122.

[16] K. Jain, J. Padhye, V. Padmanabhan, L. Qiu, Impact of interference on multi-hop wireless network performance, in: ACM MobiCom, 2003.

[17] X. Lin, N. B. Shroff, The impact of imperfect scheduling on cross-layer congestion control in wireless networks, IEEE/ACM Transactions on Networking 14 (2) (2006) 302–315.

[18] L. Jiang, J. Walrand, Stability and delay of distributed scheduling algorithms for networks of conflicting queues, Queueing Systems 72 (2012) 161–187.

[19] A. Kumar, D. Manjunath, J. Kuri, Communication Networking, Morgan Kaufmann Publishers, 2004.

[20] M. J. Neely, Stochastic Network Optimization with Application to Communication and Queueing Systems, Morgan & Claypool, 2010.

[21] Cyan, http://www.cyantechnology.com/apps/index.php.

[22] B. Aghaei, Using wireless sensor network in water, electricity and gas industry, in: 3rd IEEE International Conference on Electronics Computer Technology, 2011, pp. 14–17.

[23] W. Whitt, The queueing network analyzer, The Bell System Technical Journal 62.

[24] S. M. Ross, Introduction to Probability Models, 9th Edition, Academic Press, 2007.

[25] V. Ramaiyan, A. Kumar, E. Altman, Fixed point analysis of single cell IEEE 802.11e wlans: Uniqueness and multistability, IEEE Transactions on Networking 16 (5) (2008) 1080–1093.

[26] R. Jain, D. M. Chiu, W. Hawe, A quantitative measure of fairness and discrimination for resource allocation in shared computer systems, Tech. Rep. TR-301, DEC Research Report (1984).

[27] W. Rudin, Principles of Mathematical Analysis, 3rd Edition, McGraw-Hill Book Company, 1976.